This is the accepted manuscript made available via CHORUS. The article has been published as:

Kinetic energy density of nearly free electrons. I. Response functionals of the external potential

William C. Witt and Emily A. Carter

Phys. Rev. B **100**, 125106 — Published 3 September 2019

DOI: 10.1103/PhysRevB.100.125106

Kinetic energy density of nearly free electrons. I: Response functionals of the external potential

William C. Witt[1] and Emily A. Carter*[2]

[1] Department of Mechanical and Aerospace Engineering, and [2]School of Engineering and Applied Science, Princeton University, Princeton, New Jersey 08544-5263

* corresponding author: eac@princeton.edu

Abstract

Free electrons have a uniform kinetic energy density (KED), which evolves into a spatially varying quantity as the electrons respond to the gradual imposition of an external potential. In this paper and a companion paper, we examine two sets of functionals for describing the local, non-negative KED that emerges after such a perturbation. In this paper, we emphasize potential functionals, deriving the first- and second-order deviations from the free-electron KED as functionals of the perturbing potential, also reconsidering the analogous functionals for the local density of states and the electron density. (In the second paper, we use these results to re-express the KED response in terms of functionals of the induced electron density.) We develop reciprocal-space formulations of the response kernels to complement previously known real-space forms. The first-order function is straightforward to obtain, but the second-order function requires considerable effort. To manage the derivations, we relate the KED response to that of the one-electron Green function, and then examine the latter in detail. Finally, we provide extensive validation of the derived response functions based on asymptotic analysis of an integral representation, numerical integration of the same generating integral, and application to the linear potential model.

I. INTRODUCTION

The local properties of free electrons, such as the electron density and the kinetic energy density (KED), are uniform throughout space. As initially free electrons respond to the imposition of a new external potential, the changes in these properties may be approximated with response functionals. Here, we consider response functionals for the local, non-negative KED defined by

$$t(\mathbf{r}) = \tfrac{1}{2}\Big[\nabla_{\mathbf{r}} \cdot \nabla_{\mathbf{r}_0} \gamma(\mathbf{r},\mathbf{r}_0)\Big]_{\mathbf{r}_0 \to \mathbf{r}} \quad , \tag{1}$$

where $\gamma(\mathbf{r},\mathbf{r}_0)$ is the reduced density matrix of a non-interacting electron system governed by the Hamiltonian $\hat{H} = -\tfrac{1}{2}\nabla^2 + \hat{v}$, where $v(\mathbf{r})$ is an external potential. (The quantity $t_L(\mathbf{r}) = t(\mathbf{r}) - \tfrac{1}{4}\nabla^2 n(\mathbf{r})$ arises from another natural definition for the KED—see the Appendix—but it does not enjoy strict non-negativity.) More specifically, we investigate the limiting case of a time-independent potential that is switched on gradually over a long period of time—the new steady-state that emerges (eventually) is encoded in the static response functionals of the unperturbed system. One expects the response functional series to converge when the perturbation is sufficiently weak; a more rigorous treatment of the conditions for convergence is not given here, but see Refs. 1 and 2 for discussion of the convergence of the underlying response series (Born series) for the Green function.

In this paper and a companion paper, we examine two distinct sets of static response functionals for the local KED. In this paper, we consider first- and second-order corrections to the free-electron KED in the form of *potential functionals*, so-named because they depend explicitly on the perturbing potential. In the second paper (Part II),[3] we use these potential functionals—together with additional ingredients and a conversion procedure pioneered by Stoddart and March[4]—to obtain an alternate set of first- and second-order *density functionals* for the KED that operate on the induced electron density and do not depend explicitly on the perturbing potential. These latter functionals will help guide the design of the more sophisticated kinetic energy functionals enabling orbital-free[5–8] density functional theory[9,10] simulations, an overarching goal.

Our analysis draws heavily on a long tradition of response functional development based on the free-electron reference system and, while our focus on the KED is a differentiating feature, the approach we adopt parallels that of numerous earlier authors. For example, potential functionals yielding the response of the electron density have long been known, along with the closely related (see below) response functionals for the total kinetic energy.[11–25] We defer a more detailed account of this earlier work to the following section and mention here only one specific result, the static Lindhard function,[11]

which is likely the best-known archetype of the category. The Lindhard function and associated potential functional—respectively, $\tilde{J}_1(\mathbf{k}_1, k_\mu)$ in our notation and Eq. (78) below—governs the first-order response of the electron density and is a ubiquitous feature in textbooks on condensed matter physics.[26–28]

In the following section, we give background material on elements of theory and prior work illustrating the origin of the response functionals. In Section III, we consider the response of the equal-position Green function—that is, $G^+(\mathbf{r},\mathbf{r},E)$, the diagonal of the retarded one-electron Green function—which suffices to determine the response of other local properties of interest. For completeness, we include full mathematical detail—readers uninterested in the derivation may skip Section III and proceed directly to Section IV, where we provide the reciprocal-space response functions that are the primary results of this paper. In Section V, we describe a multi-part validation strategy confirming that the (rather complicated) second-order formulas are correct. We make concluding remarks in Section VI. An Appendix gives additional details and Supplemental Material (SM)[29] provides additional verification of the response function formulas.

II. BACKGROUND

We consider a three-dimensional system of non-interacting electrons with Hamiltonian $\hat{H} = -\frac{1}{2}\nabla^2 + \hat{v}$, where the static external potential is partitioned into a free part and a perturbation, $v(\mathbf{r}) = v_0 + v_\Delta(\mathbf{r})$. Neglecting spin-polarization for simplicity, we work in the zero-temperature grand canonical ensemble, meaning that states with energies below a chemical potential μ are each populated with two electrons. Finally, in part to avoid working with wave functions explicitly, we adopt a Green function approach.

The retarded Green function for this system is defined formally as[30,31]

$$G^+(\mathbf{r},\mathbf{r}_0,E) = \left\langle \mathbf{r} \middle| \frac{1}{E - \hat{H} + i\acute{U}} \middle| \mathbf{r}_0 \right\rangle, \tag{2}$$

which reflects the fact that $G^+(\mathbf{r},\mathbf{r}_0,E)$ is the position-space representation of an operator, $\hat{G}^+(E)$, satisfying the equation

$$(E - \hat{H} + i\acute{U})\hat{G}^+(E) = \hat{1}. \tag{3}$$

The $+i\acute{U}$ term in Eqs. (2)-(3), where $\acute{U}$ is a real, positive constant, ensures that $G^+(\mathbf{r},\mathbf{r}_0,E)$ has the intended behavior in the time-domain—specifically, that it describes propagation forward in time—and the implied limit $\acute{U} \to 0^+$ is taken at the end of any calculation of physical quantities. The function

$G^+(\mathbf{r},\mathbf{r}_0,E)$ encodes all local properties of interest, including the spin-summed local density of states (LDOS),[30,31]

$$\rho(\mathbf{r},E) = -\tfrac{2}{\pi}\Big[\,\mathrm{Im}G^+(\mathbf{r},\mathbf{r}_0,E)\Big]_{\mathbf{r}_0\to\mathbf{r}} \quad , \tag{4}$$

the electron density,

$$\begin{aligned} n(\mathbf{r}) &= -\tfrac{2}{\pi}\int_{-\infty}^{\mu}\Big[\,\mathrm{Im}G^+(\mathbf{r},\mathbf{r}_0,E)\Big]_{\mathbf{r}_0\to\mathbf{r}}\mathrm{d}E \\ &= \int_{-\infty}^{\mu}\rho(\mathbf{r},E)\mathrm{d}E \end{aligned} \quad , \tag{5}$$

and the non-negative KED introduced above,

$$\begin{aligned} t(\mathbf{r}) &= -\tfrac{2}{\pi}\int_{-\infty}^{\mu}\Big[\tfrac{1}{2}\nabla_{\mathbf{r}}\cdot\nabla_{\mathbf{r}_0}\mathrm{Im}G^+(\mathbf{r},\mathbf{r}_0,E)\Big]_{\mathbf{r}_0\to\mathbf{r}}\mathrm{d}E \\ &= \int_{-\infty}^{\mu}E\rho(\mathbf{r},E)\mathrm{d}E - v(\mathbf{r})n(\mathbf{r}) + \tfrac{1}{4}\nabla^2 n(\mathbf{r}) \end{aligned} \quad . \tag{6}$$

The second line in Eq. (6) will prove crucial in our development below—see the Appendix for a brief demonstration of its equivalence with the first line.

Unfortunately, the difficulty of obtaining the exact $G^+(\mathbf{r},\mathbf{r}_0,E)$ is akin to that of solving the Schrödinger equation itself. For this reason, we proceed by inspecting the solution for the simpler free-electron case, where $v_\Delta(\mathbf{r}) = 0$, and then afterwards summarize the iterative technique that yields approximations for the general case.

Free-electron systems and the Thomas-Fermi approximation

A free-electron system is characterized by the Hamiltonian $\hat{H}_0 = -\tfrac{1}{2}\nabla^2 + v_0$, where v_0 is a constant, and its Green function is diagonal in the momentum representation:[30,31]

$$\left\langle \mathbf{k}\right|\frac{1}{E-\hat{H}_0+i\acute{\mathrm{U}}}\left|\mathbf{k}_0\right\rangle = \tilde{G}_0^+(\mathbf{k},E)\left\langle \mathbf{k}\middle|\mathbf{k}_0\right\rangle, \tag{7}$$

where

$$\tilde{G}_0^+(\mathbf{k},E) = \frac{2}{k_E^2 - k^2 + i\acute{\mathrm{U}}_2}, \tag{8}$$

$k_E = [2(E - v_0)]^{1/2}$, and $\acute{U}_2 = 2\acute{U}$. When defining k_E we specify the principal square root such that k_E equals $i[2(v_0 - E)]^{1/2}$ when $E < v_0$. Using Eqs. (7) and (8) to compute the position representation for the free-electron Green function, one obtains

$$G_0^+(\mathbf{r}, \mathbf{r}_0, E) = -\frac{1}{2\pi} \frac{\exp\left(ik_E |\mathbf{r} - \mathbf{r}_0|\right)}{|\mathbf{r} - \mathbf{r}_0|} \tag{9}$$

following the $\acute{U} \to 0^+$ limit. Note that when $E > v_0$, the function $G_0^+(\mathbf{r}, \mathbf{r}_0, E)$ is complex-valued and oscillatory, but when $E < v_0$ it becomes purely real-valued and decays exponentially with the distance $|\mathbf{r} - \mathbf{r}_0|$.

We can apply Eqs. (4)-(6) to this result to determine the free-electron LDOS, which is zero for $E < v_0$, as well as the associated electron density and KED, which are zero for $\mu < v_0$. When nonzero, the three quantities are

$$\begin{Bmatrix} \rho_0(E) \\ n_0 \\ t_0 \end{Bmatrix} = \begin{Bmatrix} k_E / \pi^2 \\ k_\mu^3 / (3\pi^2) \\ k_\mu^5 / (10\pi^2) \end{Bmatrix}, \tag{10}$$

where $k_\mu = [2(\mu - v_0)]^{1/2}$ is typically referred to as the Fermi wave vector.

It is useful at this stage to consider the replacement $v_0 \to v(\mathbf{r})$ made everywhere in Eq. (10). This procedure yields the Thomas-Fermi[32,33] potential-functional approximations to $\rho(\mathbf{r}, E)$, $n(\mathbf{r})$, and $t(\mathbf{r})$, which, roughly speaking, are valid when $v(\mathbf{r})$ is nearly constant in the neighborhood of $\mathbf{r}$. Furthermore, recalling the partitioning $v(\mathbf{r}) = v_0 + v_\Delta(\mathbf{r})$, it is instructive to invoke the Thomas-Fermi approximation and then record Taylor series expansions about $v_\Delta(\mathbf{r}) = 0$ through second order:

$$\begin{Bmatrix} \rho_{TF}(\mathbf{r}, E) \\ n_{TF}(\mathbf{r}) \\ t_{TF}(\mathbf{r}) \end{Bmatrix} \approx \begin{Bmatrix} \rho_0(E) \\ n_0 \\ t_0 \end{Bmatrix} + \begin{Bmatrix} -1/(\pi^2 k_E) \\ -k_\mu / \pi^2 \\ -k_\mu^3 / (2\pi^2) \end{Bmatrix} v_\Delta(\mathbf{r}) + \begin{Bmatrix} -1/(2\pi^2 k_E^3) \\ 1/(2\pi^2 k_\mu) \\ 3k_\mu / (4\pi^2) \end{Bmatrix} v_\Delta(\mathbf{r})^2 . \tag{11}$$

This procedure anticipates results appearing later in Section IV: the first- and second-order coefficients appearing in Eq. (11) agree precisely with the values of the full-fledged response functions evaluated for the limiting case of a slowly varying perturbation.

Perturbation theory based on a free-electron model

Beginning from the Lippmann-Schwinger-Dyson equation that relates $\hat{G}^{+}(E)$ and $\hat{G}_0^{+}(E)$,[30,31]

$$\hat{G}^{+}(E) = \hat{G}_0^{+}(E) + \hat{G}_0^{+}(E)\hat{v}_{\Delta}\hat{G}^{+}(E), \tag{12}$$

one may repeatedly insert its left-hand side into its right-hand side to generate the infinite series,

$$\hat{G}^{+}(E) = \hat{G}_0^{+}(E) + \sum_{m=1}^{\infty} \hat{G}_0^{+}(E) \prod\nolimits_{\alpha=1}^{m} [\hat{v}_{\Delta}\hat{G}_0^{+}(E)], \tag{13}$$

where the m th order term is interpreted as free-electron propagation punctuated by m interactions with the perturbing potential $\hat{v}_{\Delta}$. We may now invoke Eqs. (4)-(6) to convert this series representation for $\hat{G}^{+}(E)$ into series expansions yielding the deviations from free-electron character in the LDOS, the electron density, and the KED:

$$\begin{Bmatrix} \rho_{\Delta}(\mathbf{r},E) \\ n_{\Delta}(\mathbf{r}) \\ t_{\Delta}(\mathbf{r}) \end{Bmatrix} = \begin{Bmatrix} \rho(\mathbf{r},E) - \rho_0(E) \\ n(\mathbf{r}) - n_0 \\ t(\mathbf{r}) - t_0 \end{Bmatrix} = \sum_{m=1}^{\infty} \begin{Bmatrix} \rho_m(\mathbf{r},E) \\ n_m(\mathbf{r}) \\ t_m(\mathbf{r}) \end{Bmatrix}. \tag{14}$$

Two equivalent formulations for the $\rho_m(\mathbf{r},E)$, $n_m(\mathbf{r})$, and $t_m(\mathbf{r})$ terms are useful. The first involves functionals of the real-space potential, $v_{\Delta}(\mathbf{r})$, and the second involves functionals of the Fourier-transformed potential, $\tilde{v}_{\Delta}(\mathbf{k})$, based on the Fourier transform conventions outlined in the Appendix.

The real-space functionals are obtained from Eqs. (4)-(6) after insertions of real-space resolutions of the identity of the form $\hat{1} = \int \mathrm{d}\mathbf{r}_{\alpha} \left|\mathbf{r}_{\alpha}\right\rangle\left\langle\mathbf{r}_{\alpha}\right|$ within the m th order term from Eq. (13). (See the following section for more detail.) The $\rho_m(\mathbf{r},E)$ are zero when $E < v_0$, which follows the fact that the free-electron Green function, Eq. (9), is purely real for this case—and accordingly, $n_m(\mathbf{r})$ and $t_m(\mathbf{r})$ are zero when $\mu < v_0$. Otherwise, the real-space functionals may be written with the following structure,

$$\begin{Bmatrix} \rho_m(\mathbf{r},E) \\ n_m(\mathbf{r}) \\ t_m(\mathbf{r}) \end{Bmatrix} = \underbrace{\cdots \int \mathrm{d}\mathbf{r}_{\alpha} \cdots}_{\substack{m \text{ integrals} \\ \alpha \in \{1,\cdots,m\}}} \begin{Bmatrix} I_m\left(\{\mathbf{r}-\mathbf{r}_{\alpha},\}_{\alpha=1}^{m} k_E\right) \\ J_m\left(\{\mathbf{r}-\mathbf{r}_{\alpha},\}_{\alpha=1}^{m} k_{\mu}\right) \\ K_m\left(\{\mathbf{r}-\mathbf{r}_{\alpha},\}_{\alpha=1}^{m} k_{\mu}\right) \end{Bmatrix} \underbrace{\cdots v_{\Delta}(\mathbf{r}_{\alpha}) \cdots}_{\substack{m \text{ potential factors} \\ \alpha \in \{1,\cdots,m\}}}. \tag{15}$$

The integral kernels appearing in Eq. (15) are the real-space response functions, for which explicit and straightforward-to-evaluate expressions are known to all orders:[4,13]

$$I_m\left(\{\mathbf{r}-\mathbf{r}_\alpha,\}_{\alpha=1}^{m}k_E\right)=\frac{(-1)^m}{(2\pi)^m\pi^2}\frac{\sin\left(k_E\sum_{\alpha=1}^{m+1}|\,\mathbf{r}_\alpha-\mathbf{r}_{\alpha-1}\,|\right)}{\prod_{\alpha=1}^{m+1}|\,\mathbf{r}_\alpha-\mathbf{r}_{\alpha-1}\,|}, \tag{16}$$

$$J_m\left(\{\mathbf{r}-\mathbf{r}_\alpha,\}_{\alpha=1}^{m}k_\mu\right)=\frac{(-1)^m k_\mu^2}{(2\pi)^m\pi^2}\frac{j_1\left(k_\mu\sum_{\alpha=1}^{m+1}|\,\mathbf{r}_\alpha-\mathbf{r}_{\alpha-1}\,|\right)}{\prod_{\alpha=1}^{m+1}|\,\mathbf{r}_\alpha-\mathbf{r}_{\alpha-1}\,|}, \tag{17}$$

and

$$\begin{aligned}K_m\left(\{\mathbf{r}-\mathbf{r}_\alpha,\}_{\alpha=1}^{m}k_\mu\right)=&\frac{(-1)^{m+1}k_\mu^4}{(2\pi)^m\pi^2}\frac{j_1''\left(k_\mu\sum_{\alpha=1}^{m+1}|\,\mathbf{r}_\alpha-\mathbf{r}_{\alpha-1}\,|\right)}{\prod_{\alpha=1}^{m+1}|\,\mathbf{r}_\alpha-\mathbf{r}_{\alpha-1}\,|}\\&-J_{m-1}\left(\{\mathbf{r}-\mathbf{r}_\alpha,\}_{\alpha=1}^{m-1}k_\mu\right)\delta(\mathbf{r}-\mathbf{r}_m)+\tfrac{1}{4}\nabla_{\mathbf{r}}^2 J_m\left(\{\mathbf{r}-\mathbf{r}_\alpha,\}_{\alpha=1}^{m}k_\mu\right)\end{aligned}, \tag{18}$$

where in Eqs. (16)-(18) we use the convention that $\mathbf{r}_0=\mathbf{r}$ and $\mathbf{r}_{m+1}=\mathbf{r}$. In Eqs. (17) and (18), respectively, $j_1(x)=(\sin x-x\cos x)/x^2$ is a spherical Bessel function and $j_1''(x)$ is the second derivative of $j_1(x)$. One may obtain the response functions for the Laplacian version of the KED (see the Appendix) by simply omitting the last term in Eq. (18).[4]

Alternatively, to develop $\rho_m(\mathbf{r},E)$, $n_m(\mathbf{r})$, and $t_m(\mathbf{r})$ as functionals of the Fourier-transformed potential, $\tilde{v}_\Delta(\mathbf{k})$, one inserts reciprocal-space resolutions of the identity of the form $\hat{1}=\int d\mathbf{k}_\alpha\,|\mathbf{k}_\alpha\rangle\langle\mathbf{k}_\alpha|$ between the operators of the m th order term from Eq. (13) before invoking Eqs. (4)-(6). These Fourier-space formulations describe the response to perturbations that are periodic in nature and are of practical utility because they facilitate more efficient evaluation of the real-space functionals with fast-Fourier-transform techniques. (In addition, the strategy employed in Part II for converting potential functionals into density functionals proceeds most naturally in reciprocal space.) After a small amount of rearrangement, the Fourier-space functionals may be written as follows:

$$\begin{Bmatrix}\rho_m(\mathbf{r},E)\\ n_m(\mathbf{r})\\ t_m(\mathbf{r})\end{Bmatrix}=\underbrace{\cdots\int\frac{d\mathbf{k}_\alpha}{(2\pi)^3}e^{i\mathbf{k}_\alpha\cdot\mathbf{r}}\cdots}_{\substack{m\text{ integrals}\\ \alpha\in\{1,\cdots,m\}}}\begin{Bmatrix}\tilde{I}_m\left(\{\mathbf{k}_\alpha,\}_{\alpha=1}^{m}k_E\right)\\ \tilde{J}_m\left(\{\mathbf{k}_\alpha,\}_{\alpha=1}^{m}k_\mu\right)\\ \tilde{K}_m\left(\{\mathbf{k}_\alpha,\}_{\alpha=1}^{m}k_\mu\right)\end{Bmatrix}\underbrace{\cdots\tilde{v}_\Delta(\mathbf{k}_\alpha)\cdots}_{\substack{m\text{ potential factors}\\ \alpha\in\{1,\cdots,m\}}}. \tag{19}$$

However, in contrast with the real-space case, straightforward-to-evaluate expressions for $\tilde{I}_m(\bullet,k_E)$, $\tilde{J}_m(\bullet,k_\mu)$, and $\tilde{K}_m(\bullet,k_\mu)$ are not known to all orders. (For compactness, we occasionally represent the wave vector arguments with a dot, $\{\mathbf{k}_\alpha,\}_{\alpha=1}^{m}\equiv\bullet$, for instances when the order m is left arbitrary.) In

principle, these functions could be obtained for any m by direct Fourier transformation of their real-space counterparts; however, the many-dimensional integrations that arise are cumbersome and nearly intractable beyond first order.[20] In the following section, we follow an alternate route to obtain the second-order functions, but even with this technique, progress at higher orders remains limited.[18,23,34–36]

As mentioned above, $\tilde{J}_1(\mathbf{k}_1, k_\mu)$ is attributed to Lindhard[11] and is widely known; in addition, one may use it to obtain $\tilde{I}_1(\mathbf{k}_1, k_E)$ by differentiation. For the second-order case, several authors provide expressions for $\tilde{J}_2(\mathbf{k}_1, \mathbf{k}_2, k_\mu)$, and to a lesser extent $\tilde{I}_2(\mathbf{k}_1, \mathbf{k}_2, k_E)$, but these functions are considerably more difficult to obtain. The earliest such derivation appears to be that of Lloyd and Sholl,[15] and one finds derivations of alternate forms scattered across the literature.[17,19,21,24] By contrast, the reciprocal-space response functions for the KED are not well-studied. (The sole example appears to be work by Li and Percus,[24] who, for one-dimensional systems only, provide reciprocal-space response functions for the KED through second order.) Here, we contribute explicit formulas for $\tilde{K}_1(\mathbf{k}_1, k_\mu)$ and $\tilde{K}_2(\mathbf{k}_1, \mathbf{k}_2, k_\mu)$ appropriate for three-dimensional systems—and, by simple extension, the analogous functions for the Laplacian version of the KED (see the Appendix)—which complement the expressions for the LDOS and electron density discussed previously. We give these results in Section IV, along with the corresponding expressions for $\tilde{I}_1(\mathbf{k}_1, k_E)$, $\tilde{I}_2(\mathbf{k}_1, \mathbf{k}_2, k_E)$, $\tilde{J}_1(\mathbf{k}_1, k_\mu)$, and $\tilde{J}_2(\mathbf{k}_1, \mathbf{k}_2, k_\mu)$— both for purposes of comparison and because we use the latter as building blocks for $\tilde{K}_1(\mathbf{k}_1, k_\mu)$ and $\tilde{K}_2(\mathbf{k}_1, \mathbf{k}_2, k_\mu)$.

Although the local quantities discussed so far are our primary focus, we conclude this background section by highlighting a connection between the response of the electron density and that of the integrated energy of the non-interacting-electron system, E_{tot}, as well as the integrated kinetic energy, T_s. We begin with a coupling constant integral for the system energy,[4,19,37–41]

$$E_{\text{tot}} - E_0 = \int_0^1 \mathrm{d}\lambda \int \mathrm{d}\mathbf{r}\, v_\Delta(\mathbf{r})\, n_\Delta^\lambda(\mathbf{r}), \tag{20}$$

in which E_{tot} is the total energy, E_0 is the energy of a free-electron system with the same number of electrons per unit volume, and $n_\Delta^\lambda(\mathbf{r})$ is the deviation from the free-electron density that would be generated by the scaled perturbation $\lambda v_\Delta(\mathbf{r})$. The expression in Eq. (20) is commonly derived using the Hellman-Feynman theorem[42] and the value of the integral is effectively the electrostatic work required to assemble the new charge distribution.[4,19] If we replace $n_\Delta^\lambda(\mathbf{r})$ in Eq. (20) with the response-functional

series appearing in Eq. (15)—remembering to attach factors of λ where appropriate—we may perform the λ integral directly to deduce that[4,19,40,41]

$$\begin{Bmatrix} E_{\text{tot}} - E_0 \\ T_s - T_0 \end{Bmatrix} = \sum_{m=1}^{\infty} \int \mathrm{d}\mathbf{r} \underbrace{\cdots \int \mathrm{d}\mathbf{r}_\alpha \cdots}_{\substack{m \text{ integrals} \\ \alpha \in \{1,\cdots,m\}}} \begin{Bmatrix} \frac{1}{m+1} J_m\left(\{\mathbf{r} - \mathbf{r}_\alpha,\}_{\alpha=1}^{m} k_\mu\right) \\ \frac{-m}{m+1} J_m\left(\{\mathbf{r} - \mathbf{r}_\alpha,\}_{\alpha=1}^{m} k_\mu\right) \end{Bmatrix} v_\Delta(\mathbf{r}) \underbrace{\cdots v_\Delta(\mathbf{r}_\alpha) \cdots}_{\substack{m \text{ potential factors} \\ \alpha \in \{1,\cdots,m\}}}, \tag{21}$$

where T_0 is an integrated kinetic energy of the free-electron reference system. The response of the kinetic energy given in Eq. (21) is obtained by subtracting the potential energy from the total energy at each order. The corresponding reciprocal space formulations are[4,19,40,41]

$$\begin{Bmatrix} E_{\text{tot}} - E_0 \\ T_s - T_0 \end{Bmatrix} = \sum_{m=1}^{\infty} \underbrace{\cdots \int \frac{\mathrm{d}\mathbf{k}_\alpha}{(2\pi)^3} \cdots}_{\substack{m \text{ integrals} \\ \alpha \in \{1,\cdots,m\}}} \begin{Bmatrix} \frac{1}{m+1} \tilde{J}_m\left(\{\mathbf{k}_\alpha,\}_{\alpha=1}^{m} k_\mu\right) \\ \frac{-m}{m+1} \tilde{J}_m\left(\{\mathbf{k}_\alpha,\}_{\alpha=1}^{m} k_\mu\right) \end{Bmatrix} \tilde{v}_\Delta(-\textstyle\sum_{\alpha=1}^{m} \mathbf{k}_\alpha) \underbrace{\cdots \tilde{v}_\Delta(\mathbf{k}_\alpha) \cdots}_{\substack{m \text{ potential factors} \\ \alpha \in \{1,\cdots,m\}}}, \tag{22}$$

which are developed in an analogous manner.

III. RESPONSE OF THE EQUAL-POSITION GREEN FUNCTION

In this section — commencing our pursuit of explicit expressions for $\tilde{K}_1(\mathbf{k}_1, k_\mu)$ and $\tilde{K}_2(\mathbf{k}_1, \mathbf{k}_2, k_\mu)$ — we investigate in greater detail the m th-order response of the equal-position Green function. Readers uninterested in the details of the derivation may skip directly to Section IV, where the results are given. The m th order equal-position Green function is defined using Eq. (13) as

$$G_m^+(\mathbf{r}, \mathbf{r}, E) = \left\langle \mathbf{r} \middle| \hat{G}_0^+(E) \underbrace{\cdots \hat{v}_\Delta \hat{G}_0^+(E) \cdots}_{\text{m repetitions}} \middle| \mathbf{r} \right\rangle. \tag{23}$$

We choose this object as a jumping-off point because of its simple structure; furthermore, as noted, response functions for $G_m^+(\mathbf{r}, \mathbf{r}, E)$ together with Eqs. (4)-(6) lead directly to response functions for the other local properties. In the spirit of Eqs. (15) and (19), we repeatedly insert real-space resolutions of the identity of the form $\hat{1} = \int \mathrm{d}\mathbf{r}_\alpha \left|\mathbf{r}_\alpha\right\rangle\left\langle\mathbf{r}_\alpha\right|$ or reciprocal-space resolutions of the identity of the form $\hat{1} = \int \mathrm{d}\mathbf{k}_\alpha \left|\mathbf{k}_\alpha\right\rangle\left\langle\mathbf{k}_\alpha\right|$ into Eq. (23) to obtain, after some rearrangement for the latter case,

$$
\begin{aligned}
G_m^+(\mathbf{r},\mathbf{r},E) &= \underbrace{\cdots\int \mathrm{d}\mathbf{r}_\alpha \cdots}_{\substack{m \text{ integrals} \\ \alpha\in\{1,\cdots,m\}}} H_m\left(\{\mathbf{r}-\mathbf{r}_\alpha,\}_{\alpha=1}^m E\right)\underbrace{\cdots v_\Delta(\mathbf{r}_\alpha)\cdots}_{\substack{m \text{ potential factors} \\ \alpha\in\{1,\cdots,m\}}} \\
&= \underbrace{\cdots\int \frac{\mathrm{d}\mathbf{k}_\alpha}{(2\pi)^3} e^{i\mathbf{k}_\alpha\cdot\mathbf{r}} \cdots}_{\substack{m \text{ integrals} \\ \alpha\in\{1,\cdots,m\}}} \tilde{H}_m\left(\{\mathbf{k}_\alpha,\}_{\alpha=1}^m E\right)\underbrace{\cdots \tilde{v}_\Delta(\mathbf{k}_\alpha)\cdots}_{\substack{m \text{ potential factors} \\ \alpha\in\{1,\cdots,m\}}},
\end{aligned}
\tag{24}
$$

where we have introduced real- and reciprocal-space response functions, $H_m(\bullet,E)$ and $\tilde{H}_m(\bullet,E)$. In doing so, we deduce immediately an analytical expression for the real-space function,

$$
H_m\left(\{\mathbf{r}-\mathbf{r}_\alpha,\}_{\alpha=1}^m E\right) = \prod_{\alpha=0}^{m} G_0^+\left(\mathbf{r}_\alpha,\mathbf{r}_{\alpha+1},E\right), \tag{25}
$$

with $\mathbf{r}_0 = \mathbf{r}_{m+1} = \mathbf{r}$, as well as a compact integral form for the reciprocal-space function,

$$
\tilde{H}_m\left(\{\mathbf{k}_\alpha,\}_{\alpha=1}^m E\right) = \int \frac{\mathrm{d}\mathbf{k}_0}{(2\pi)^3} \prod_{\beta=0}^{m} \tilde{G}_0^+\left(\sum\nolimits_{\alpha=0}^{\beta}\mathbf{k}_\alpha, E\right). \tag{26}
$$

The integral in Eq. (26) prevents one from easily computing the numerical value of $\tilde{H}_m(\bullet,E)$ for a given set of arguments. However, in contrast to the inconvenient representation of $\tilde{H}_m(\bullet,E)$ provided by the $3m$-dimensional Fourier transform of $H_m(\bullet,E)$, Eq. (26) involves only a single, three-dimensional integral, irrespective of the order. Integrals resembling Eq. (26) arise frequently in theoretical physics.[17,25,34–36]

The bulk of this section is devoted to completing the integral in Eq. (26) for the first- and second-order cases, yielding $\tilde{H}_1(\mathbf{k}_1,E)$ and $\tilde{H}_2(\mathbf{k}_1,\mathbf{k}_2,E)$ in analytical form. With knowledge of these functions, we may use

$$
\tilde{I}_m(\bullet,k_E) = -\tfrac{2}{\pi}\,\mathrm{Im}\tilde{H}_m(\bullet,E), \tag{27}
$$

$$
\tilde{J}_m(\bullet,k_\mu) = \int_{-\infty}^{\mu} \tilde{I}_m(\bullet,k_E)\mathrm{d}E, \tag{28}
$$

and

$$
\begin{aligned}
\tilde{K}_m(\bullet,k_\mu) &= \int_{-\infty}^{\mu}(E-v_0)\tilde{I}_m(\bullet,k_E)\mathrm{d}E - \mathrm{S}_m\left\{\tilde{J}_{m-1}(\bullet,k_\mu)\right\} - \tfrac{1}{4}\|\sum\nolimits_{\alpha=1}^{m}\mathbf{k}_\alpha\|^2\,\tilde{J}_m(\bullet,k_\mu) \\
&= -\int_{-\infty}^{\mu}\tilde{J}_m(\bullet,k_E)\mathrm{d}E - \mathrm{S}_m\left\{\tilde{J}_{m-1}(\bullet,k_\mu)\right\} + \left[\tfrac{1}{2}k_\mu^2 - \tfrac{1}{4}\|\sum\nolimits_{\alpha=1}^{m}\mathbf{k}_\alpha\|^2\right]\tilde{J}_m(\bullet,k_\mu),
\end{aligned}
\tag{29}
$$

which derive from Eqs. (4)-(6), to construct corresponding response functions for the LDOS, electron density, and the KED — the results of this procedure are recorded later in Section IV.

Four points of clarification are in order. First, the process of deducing Eq. (27) involves noting that $v_{\Delta}(\mathbf{r})$ is purely real and recognizing that, because $H_m(\bullet,E)$ is an even function in its position arguments, its imaginary part determines completely the imaginary part of its Fourier transform, $\tilde{H}_m(\bullet,E)$. Second, the optional symmetrization instruction in Eq. (29) is illustrated by the example $\mathrm{S}_2\{\tilde{J}_1(\mathbf{k}_1,k_\mu)\}=\frac{1}{2}[\tilde{J}_1(\mathbf{k}_1,k_\mu)+\tilde{J}_1(\mathbf{k}_2,k_\mu)]$. Third, the second line in Eq. (29) is obtained from the first line following an integration by parts. Finally, the response functions for the Laplacian version of the KED are obtained by adding $\| \sum_{\alpha=1}^{m}\mathbf{k}_\alpha \|^2 \, \tilde{J}_m(\bullet,k_\mu)\big/4$ to Eq. (29).

First-order

The linear response of the equal-position Green function is governed by

$$\tilde{H}_1(\mathbf{k}_1,E)=\int\frac{\mathrm{d}\mathbf{k}_0}{(2\pi)^3}\frac{2}{k_E^2-k_0^2+i\acute{\mathrm{U}}}\frac{2}{k_E^2-\|\mathbf{k}_0+\mathbf{k}_1\|^2+i\acute{\mathrm{U}}}. \tag{30}$$

One may attack this integral in several ways; we choose an approach that foreshadows our strategy for the more difficult second-order case. We begin by noting that for $\mathbf{k}_1=0$ we encounter a multiple of the generic integral

$$\begin{aligned}\int\frac{\mathrm{d}\mathbf{k}_0}{(2\pi)^3}\frac{1}{[x-k_0^2+i\acute{\mathrm{U}}]^2}&=\frac{1}{2\pi^2}\int_0^\infty \mathrm{d}k_0\frac{k_0^2}{[x-k_0^2+i\acute{\mathrm{U}}]^2}\\&=\frac{1}{4\pi^2}\int_{-\infty}^{\infty}\mathrm{d}k_0\frac{k_0^2}{(k_0+[x+i\acute{\mathrm{U}}]^{1/2})^2(k_0-[x+i\acute{\mathrm{U}}]^{1/2})^2},\\&=\frac{i}{8\pi}\frac{1}{[x+i\acute{\mathrm{U}}]^{1/2}}\end{aligned} \tag{31}$$

with x as a real number. This integral will reappear several times below; the result in the final line may be obtained by application of the residue theorem. For concreteness, we specify that the square root on the right hand side of Eq. (31) refers to the principal branch with a cut along the negative real axis. Using this result, we conclude that

$$\tilde{H}_1(0,E)=\frac{i}{2\pi k_E}, \tag{32}$$

following the $\acute{\mathrm{U}}\to 0^+$ limit.

To proceed more generally, we combine the two denominators in Eq. (30) using the formula

$$\frac{1}{A_1 A_2} = \int_0^1 \mathrm{d}x \frac{1}{[(1-x)A_1 + xA_2]^2}; \tag{33}$$

in the new denominator, we complete the square with all terms involving $\mathbf{k}_0$ before shifting the origin for the $\mathbf{k}_0$ integral with the replacement $\mathbf{k}_0 \to \mathbf{k}_0 - x\mathbf{k}_1$, eventually obtaining

$$\tilde{H}_1(\mathbf{k}_1, E) = \int_0^1 \mathrm{d}x \int \frac{\mathrm{d}\mathbf{k}_0}{(2\pi)^3} \frac{4}{[k_E^2 - (x - x^2)k_1^2 - k_0^2 + i\acute{U}_2]^2}. \tag{34}$$

At this point, we invoke Eq. (31) to generate

$$\tilde{H}_1(\mathbf{k}_1, E) = \frac{i}{2\pi} \int_0^1 \mathrm{d}x \frac{1}{[k_E^2 - (x - x^2)k_1^2 + i\acute{U}_2]^{1/2}}; \tag{35}$$

then, noting that the integrand remains analytic over the full integration path, we make the Euler substitution $[k_E^2 - (x - x^2)k_1^2 + i\acute{U}_2]^{1/2} = -k_1 x + t$, to reduce Eq. (35) to the more tractable form

$$\tilde{H}_1(\mathbf{k}_1, E) = \frac{i}{2\pi k_1} \int_{[k_E^2 + i\acute{U}_2]^{1/2}}^{[k_E^2 + i\acute{U}_2]^{1/2} + k_1} \mathrm{d}t \frac{1}{t - \frac{1}{2}k_1}. \tag{36}$$

The final integral yields

$$\tilde{H}_1(\mathbf{k}_1, E) = \frac{i}{2\pi k_1} \left[\mathrm{Ln}\left([k_E^2 + i\acute{U}_2]^{1/2} + \tfrac{1}{2}k_1 \right) - \mathrm{Ln}\left([k_E^2 + i\acute{U}_2]^{1/2} - \tfrac{1}{2}k_1 \right) \right], \tag{37}$$

where $\mathrm{Ln}(z)$ is the principal logarithm with branch cut along the negative real axis. After careful extraction of the $\acute{U} \to 0^+$ limit, we obtain

$$\tilde{H}_1(\mathbf{k}_1, E) = \begin{Bmatrix} \frac{1}{\pi k_1} \arctan\left(\frac{k_1}{2[|k_E^2|]^{1/2}} \right) & E < v_0 \\ \frac{h(k_1 - 2k_E)}{2k_1} + \frac{i}{2\pi k_1} \ln\left| \frac{k_1 + 2k_E}{k_1 - 2k_E} \right| & E > v_0 \end{Bmatrix}, \tag{38}$$

where the range of $\arctan(x)$ for real x is $(-\pi/2, \pi/2)$ and $h(x)$ is the Heaviside step function. Note that Eq. (32) is recovered in the $k_1 \to 0$ limit.

Second-order

The quadratic response of the equal-position Green function is governed by

$$\tilde{H}_2(\mathbf{k}_1, \mathbf{k}_2, E) = \int \frac{\mathrm{d}\mathbf{k}_0}{(2\pi)^3} \frac{2}{k_E^2 - k_0^2 + i\acute{U}_2} \frac{2}{k_E^2 - \| \mathbf{k}_0 + \mathbf{k}_1 \|^2 + i\acute{U}_2} \frac{2}{k_E^2 - \| \mathbf{k}_0 + \mathbf{k}_1 + \mathbf{k}_2 \|^2 + i\acute{U}_2}. \tag{39}$$

This integral requires more finesse and inventiveness than its first-order counterpart. We begin by considering simplifications that arise in a few special cases before eventually tackling it for arbitrary wave vectors. For the latter task, we adapt the elegant approach of Brovman and Kholas.[18]

Simplified case: When $\mathbf{k}_1 = 0$ *and* $\mathbf{k}_2 = 0$

When both $\mathbf{k}_1$ and $\mathbf{k}_2$ are zero, we may write Eq. (39) in the form

$$\tilde{H}_2(\mathbf{k}_1, \mathbf{k}_2, E) = -2\frac{\partial}{\partial E}\int \frac{\mathrm{d}\mathbf{k}_0}{(2\pi)^3}\frac{1}{[k_E^2 - k_0^2 + i\acute{U}]^2}, \tag{40}$$

invoke Eq. (31), and then take the $\acute{U} \to 0^+$ limit to obtain

$$\tilde{H}_2(0,0,E) = \frac{i}{4\pi k_E^3}. \tag{41}$$

Simplified case: When $\mathbf{k}_1 = 0$, $\mathbf{k}_2 = 0$, *or* $\mathbf{k}_2 = -\mathbf{k}_1$

If one of the wave vector arguments is zero, or if $\mathbf{k}_2 = -\mathbf{k}_1$, then Eq. (39) may be written (some manipulation is necessary when $\mathbf{k}_2 = 0$)

$$\tilde{H}_2(\mathbf{k}_1, 0, E) = \tilde{H}_2(0, \mathbf{k}_1, E) = \tilde{H}_2(\mathbf{k}_1, -\mathbf{k}_1, E) = \int \frac{\mathrm{d}\mathbf{k}_0}{(2\pi)^3}\frac{4}{[k_E^2 - k_0^2 + i\acute{U}]^2}\frac{2}{k_E^2 - \|\mathbf{k}_0 + \mathbf{k}_1\|^2 + i\acute{U}}. \tag{42}$$

By comparing Eq. (42) with Eq. (30), one may verify that the following relationship holds after some rearrangement

$$\tilde{H}_2(\mathbf{k}_1, 0, E) = \tilde{H}_2(0, \mathbf{k}_1, E) = \tilde{H}_2(\mathbf{k}_1, -\mathbf{k}_1, E) = -\frac{1}{2}\frac{\partial}{\partial E}\tilde{H}_1(\mathbf{k}_1, E), \tag{43}$$

which leads directly to the result

$$\tilde{H}_2(\mathbf{k}_1, 0, E) = \tilde{H}_2(0, \mathbf{k}_1, E) = \tilde{H}_2(\mathbf{k}_1, -\mathbf{k}_1, E) = \begin{Bmatrix} -\dfrac{1}{\pi[|k_E^2|]^{1/2}}\dfrac{1}{k_1^2 + 4|k_E^2|} & E < v_0 \\ \dfrac{\delta(k_1 - 2k_E)}{2k_1 k_E} - \dfrac{i}{\pi k_E}\dfrac{1}{k_1^2 - 4k_E^2} & E > v_0 \end{Bmatrix}. \tag{44}$$

General case: Preliminary considerations

It is useful at this stage to introduce the triangle formed by $\mathbf{k}_1$, $\mathbf{k}_2$, and a third vector $\mathbf{k}_3 = -(\mathbf{k}_1 + \mathbf{k}_2)$, which features prominently in the coming analysis. The circumradius, k_R, of this triangle may be computed with the formulas

$$k_R = \frac{k_1 k_2 k_3}{4 \cdot \text{area}} = \frac{k_\alpha}{2 \sin \theta_\alpha}, \tag{45}$$

where $\alpha \in \{1,2,3\}$ and θ_α is the interior angle opposite side k_α. We also define, for compactness in the expressions that follow,

$$c_\alpha = \cos \theta_\alpha = -\mathbf{k}_\beta \cdot \mathbf{k}_\gamma / (k_\beta k_\gamma), \tag{46}$$

where (α, β, γ) is a cyclic permutation of $\{1,2,3\}$. In the limiting case where $\mathbf{k}_1$ and $\mathbf{k}_2$ become collinear, the triangle collapses, $k_R \to \infty$, and $c_\alpha \to \pm 1$.

To evaluate $\tilde{H}_2(\mathbf{k}_1, \mathbf{k}_2, E)$ for the general case, we begin by employing the formula

$$\frac{1}{A_1 A_2 A_3} = 2! \int_0^1 \mathrm{d}x \int_0^1 \mathrm{d}y \frac{h(1-x-y)}{[(1-x-y)A_1 + xA_2 + yA_3]^3}, \tag{47}$$

to combine the three denominators in Eq. (39). In the unified denominator, we complete the square with all terms involving $\mathbf{k}_0$ and then shift the origin of the $\mathbf{k}_0$ integral with the replacement $\mathbf{k}_0 \to \mathbf{k}_0 - x\mathbf{k}_1 + y\mathbf{k}_3$ to write Eq. (39) in the form

$$\tilde{H}_2(\mathbf{k}_1, \mathbf{k}_2, E) = 16 \int_0^1 \mathrm{d}x \int_0^1 \mathrm{d}y \int \frac{\mathrm{d}\mathbf{k}_0}{(2\pi)^3} \frac{h(1-x-y)}{[k_E^2 - k_0^2 + \| x\mathbf{k}_1 - y\mathbf{k}_3 \|^2 - xk_1^2 - yk_3^2 + i0^+]^3}. \tag{48}$$

We now re-write Eq. (48) as

$$\tilde{H}_2(\mathbf{k}_1, \mathbf{k}_2, E) = -4 \frac{\partial}{\partial E} \int_0^1 \mathrm{d}x \int_0^1 \mathrm{d}y \int \frac{\mathrm{d}\mathbf{k}_0}{(2\pi)^3} \frac{h(1-x-y)}{[k_E^2 - xk_1^2 - yk_3^2 + \| x\mathbf{k}_1 - y\mathbf{k}_3 \|^2 - k_0^2 + i0^+]^2}, \tag{49}$$

so that we may invoke Eq. (31) to complete the $\mathbf{k}_0$ integral; afterwards, we perform the energy derivative to obtain

$$\tilde{H}_2(\mathbf{k}_1, \mathbf{k}_2, E) = \frac{i}{2\pi} \int_0^1 \mathrm{d}x \int_0^1 \mathrm{d}y \frac{h(1-x-y)}{[k_E^2 - xk_1^2 - yk_3^2 + \| x\mathbf{k}_1 - y\mathbf{k}_3 \|^2 + i0^+]^{3/2}}, \tag{50}$$

recalling that the principal square root is intended.

Eq. (50) is an exact reformulation of Eq. (39), and one may verify that the results given in the previous subsections are recovered from Eq. (50) when one or all of $\mathbf{k}_1$, $\mathbf{k}_2$, and $\mathbf{k}_3$ are set to zero. More importantly, Eq. (50) represents an improvement over Eq. (39) in several respects: the integrand contains only a single denominator and the integration consists of a double integral over a unit square rather than a triple integral over an infinite domain. We leverage this latter observation in Section V below, where we develop a numerical scheme for validating our analytical formulas.

The double integral appearing Eq. (50) belongs to a class of integrals that are deceptively difficult to perform. Over time, a range of techniques have been developed for such problems.[17,18,34–36] The approach of Brovman and Kholas is particularly well-suited for the task because it preserves important symmetries during all intermediate steps. We adapt this technique to our problem after a brief aside.

Simplified case: When $\mathbf{k}_1$, $\mathbf{k}_2$, and $\mathbf{k}_3$ form a small equilateral triangle

We consider now the case when $\mathbf{k}_1$, $\mathbf{k}_2$, and $\mathbf{k}_3$ form an equilateral triangle of with sides of length l, such that $\mathbf{k}_1 \cdot \mathbf{k}_3 = -l^2/2$. In this case, the function $\tilde{H}_2(\mathbf{k}_1, \mathbf{k}_2, k_E)$ depends on a single parameter, l, and we may write

$$\tilde{H}_2^{\text{equilateral}}(l, E) = \frac{i}{2\pi} \int_0^1 \mathrm{d}x \int_0^1 \mathrm{d}y \frac{h(1-x-y)}{[k_E^2 - l^2(x - x^2 - xy - y^2 + y) + i0^+]^{3/2}}. \tag{51}$$

Even with this simplification, the x and y integrals remain nontrivial; however, if we introduce a small-l series approximation of the form

$$\frac{1}{[z - l^2 a]^{3/2}} \approx \frac{1}{z^{3/2}} + \frac{3a}{2z^{5/2}} l^2 + \frac{15a^2}{8z^{7/2}} l^4, \tag{52}$$

the x and y integrals become elementary, yielding the asymptotic result

$$\tilde{H}_2^{\text{equilateral}}(l \to 0, E) \approx \frac{i}{4\pi k_E^3} \left[1 + \frac{3}{2} \frac{l^2}{4k_E^2} + 2 \frac{l^4}{16 k_E^4} \right]. \tag{53}$$

Note that Eq. (53) reduces to Eq. (41) in the $l \to 0$ limit, as expected. More significantly, the limiting form given by Eq. (53) is a required feature of the general analytical expression for $\tilde{H}_2(\mathbf{k}_1, \mathbf{k}_2, E)$, providing an important consistency check. Later, in Section V, we develop related asymptotic expressions for the LDOS, electron density, and KED for validation purposes.

General case: Completing the derivation

We resume consideration of the general case by writing Eq. (50) in the form — recalling the definition $\mathbf{k}_3 = -(\mathbf{k}_1 + \mathbf{k}_2)$ —

$$\tilde{H}_2(\mathbf{k}_1, \mathbf{k}_2, E) = \frac{i}{2\pi} \iint_{\mathrm{Z}} \mathrm{d}x\mathrm{d}y \frac{1}{[k_E^2 - xk_1^2 - yk_3^2 + \| x\mathbf{k}_1 - y\mathbf{k}_3 \|^2 + i0^+]^{3/2}}, \tag{54}$$

where the region of integration, Z, is the triangle shown in Fig. 1(a). As x and y range over Z, the vector $x\mathbf{k}_1 - y\mathbf{k}_3$ traverses a triangular region in space with side lengths k_1, k_2, and k_3. This observation suggests that our task may become simpler if we make a transformation of variables that maps Z to a region with those side lengths. The transformation $(x, y) \to (p, q)$ given by

$$\begin{pmatrix} p \\ q \end{pmatrix} = \begin{bmatrix} k_1 & -\frac{\mathbf{k}_1 \cdot \mathbf{k}_3}{k_1} \\ 0 & \frac{k_2 k_3}{2k_R} \end{bmatrix} \begin{pmatrix} x \\ y \end{pmatrix} \tag{55}$$

maps Z to the region R shown in Fig. 1(b). After solving Eq. (55) to obtain

$$\begin{pmatrix} x \\ y \end{pmatrix} = \begin{bmatrix} \frac{1}{k_1} & \frac{2k_R \mathbf{k}_1 \cdot \mathbf{k}_3}{k_1^2 k_2 k_3} \\ 0 & \frac{2k_R}{k_2 k_3} \end{bmatrix} \begin{pmatrix} p \\ q \end{pmatrix} \tag{56}$$

and accounting for the Jacobian of the transformation, we recast Eq. (54) into

$$\tilde{H}_2(\mathbf{k}_1, \mathbf{k}_2, E) = \frac{i}{\pi} \frac{k_R}{k_1 k_2 k_3} \iint_{\mathrm{R}} \mathrm{d}p\mathrm{d}q \frac{1}{[k_E^2 + p^2 - k_1 p + q^2 - 2c_1 k_R q + i0^+]^{3/2}} \tag{57}$$

following a fair bit of simplification. Next, we complete the square for both p and q to obtain

$$\tilde{H}_2(\mathbf{k}_1, \mathbf{k}_2, E) = \frac{i}{\pi} \frac{k_R}{k_1 k_2 k_3} \iint_{\mathrm{R}} \mathrm{d}p\mathrm{d}q \frac{1}{[k_E^2 - k_R^2 + (p - \frac{1}{2}k_1)^2 + (q - c_1 k_R)^2 + i0^+]^{3/2}}. \tag{58}$$

This form suggests the possibility of another coordinate change, $(p, q) \to (u, v)$, where $u = p - \frac{1}{2}k_1$ and $v = q - c_1 k_R$. Before doing so, we inspect the point $(p, q) = (\frac{1}{2}k_1, c_1 k_R)$, which — underscoring the aspects of symmetry involved — is the circumcenter of R, as one may readily verify by computing the distances between it and the three vertices. Accordingly, we write

$$\tilde{H}_2(\mathbf{k}_1, \mathbf{k}_2, E) = \frac{i}{\pi} \frac{k_R}{k_1 k_2 k_3} \iint_{\mathrm{W}} \mathrm{d}u\mathrm{d}v \frac{1}{[k_E^2 - k_R^2 + u^2 + v^2 + i0^+]^{3/2}}, \tag{59}$$

where the region W, shown in Fig. 1(c), differs from R only by a translation that locates the circumcenter of W at the origin of the uv axes.

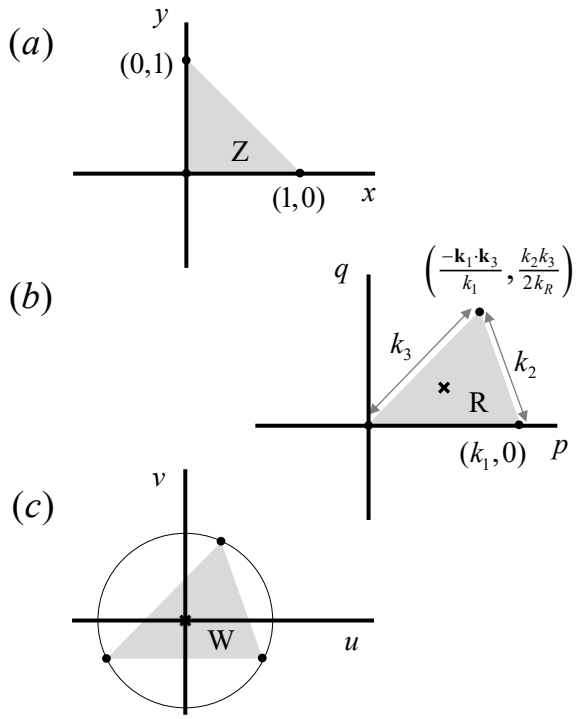

FIG. 1. Diagrams of *(a)* the triangle Z in the xy plane, which is the region of integration introduced in Eq. (54); *(b)* the triangle R in the pq plane, which is the region of integration introduced in Eq. (57); and *(c)* the triangle W in the uv plane, which is the region of integration introduced in Eq. (59). In *(b)*, the x marks the circumcenter of R. The regions W and R are identical in size, but the circumcenter of W coincides with the origin of the uv axes.

Our manipulations thus far have been building towards a change to polar coordinates, (r,φ), in the uv plane, after which Eq. (59) becomes

$$\tilde{H}_2(\mathbf{k}_1,\mathbf{k}_2,E)=\frac{i}{\pi}\frac{k_R}{k_1k_2k_3}\iint_{\mathrm{W}}\mathrm{d}r\mathrm{d}\varphi\frac{r}{[k_E^2-k_R^2+r^2+i\Gamma_2]^{3/2}}. \tag{60}$$

To manage the integration over W, we express the full integral as a sum of integrals over more elementary regions — see Fig. 2 — to obtain

$$\tilde{H}_2(\mathbf{k}_1,\mathbf{k}_2,E)=\frac{i}{\pi}\frac{k_R}{k_1k_2k_3}\sum_{\alpha=1}^{3}\mathrm{sgn}(c_\alpha)\int_{-\varphi_\alpha^{\max}}^{\varphi_\alpha^{\max}}\mathrm{d}\varphi\int_0^{r_\alpha^{\max}(\varphi)}\mathrm{d}r\,\frac{r}{[k_E^2-k_R^2+r^2+i0^+]^{3/2}} \tag{61}$$

with

$$\begin{aligned}\varphi_\alpha^{\max}&=\arcsin\left(\frac{k_\alpha}{2k_R}\right)\\ r_\alpha^{\max}(\varphi)&=\frac{[k_R^2-\frac{1}{4}k_\alpha^2]^{1/2}}{\cos\varphi}\end{aligned}. \tag{62}$$

The sign functions appearing in Eq. (61) arise because the circumcenter of an obtuse triangle lies outside of the triangle itself (see Fig. 2). If W is acute, the sign functions will all return $+1$. If W is obtuse, the sign function associated with the obtuse angle will return -1. Somewhat subtly, it is also the case that

$$\begin{aligned}\varphi_\alpha^{\max}&=\arcsin\left(\sin\theta_\alpha\right)\\ &=\theta_\alpha h(c_\alpha)+(\pi-\theta_\alpha)h(-c_\alpha)\end{aligned}, \tag{63}$$

which is related to the geometrical constraint $\varphi_\alpha^{\max}\le\pi/2$.

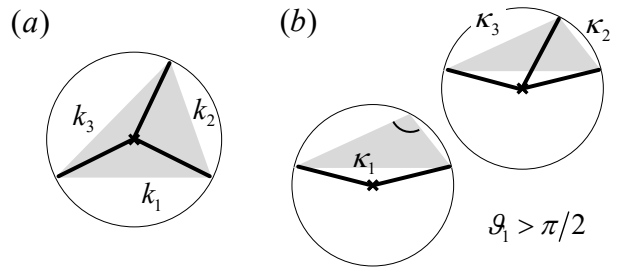

FIG. 2. Diagrams facilitating the transition from Eq. (60) to Eq. (61). In *(a)*, the integration region (shaded) is a triangle with side lengths k_1, k_2, and k_3. All angles are acute and therefore the triangle's circumcenter lies within its interior. To facilitate the integration, the shaded region is partitioned into three isosceles triangles, each having two sides of length k_R, the triangle's circumradius (dark lines), and one side of length k_α (where $\alpha\in\{1,2,3\}$). In *(b)*, the integration region is a different triangle with side lengths κ_1, κ_2, and κ_3. The angle ϑ_1 (opposite κ_1) is obtuse and therefore the triangle's circumcenter lies outside its interior. The integration is managed by subtracting the integral

over isosceles triangle associated with κ_1 from the sum of those associated with κ_2 and κ_3.

The remaining task is to evaluate the double integrals of the form

$$\int_{-\varphi_\alpha^{\max}}^{\varphi_\alpha^{\max}} \mathrm{d}\varphi \int_0^{r_\alpha^{\max}(\varphi)} \mathrm{d}r \frac{r}{[k_E^2 - k_R^2 + r^2 + i\acute{U}_2]^{3/2}}. \tag{64}$$

The r integral is completed easily and the result may be expressed as

$$\frac{2\varphi_\alpha^{\max}}{[k_E^2 - k_R^2 + i\acute{U}_2]^{1/2}} - \int_{-\varphi_\alpha^{\max}}^{\varphi_\alpha^{\max}} \mathrm{d}\varphi \frac{|\cos\varphi|}{[(k_E^2 - k_R^2 + i\acute{U}_2)\cos^2\varphi + k_R^2 - \tfrac{1}{4}k_\alpha^2]^{1/2}}. \tag{65}$$

Because $\varphi_\alpha^{\max} \le \pi/2$, the absolute value signs in the numerator of this expression are in fact unnecessary. Introducing $t = \sin\varphi$ and leveraging the symmetry of the remaining integrand, we write the previous result as

$$\frac{2\varphi_\alpha^{\max}}{[k_E^2 - k_R^2 + i\acute{U}_2]^{1/2}} - 2\int_0^{k_\alpha/(2k_R)} \mathrm{d}t \frac{1}{[(k_E^2 - k_R^2 + i\acute{U}_2)(1-t^2) + k_R^2 - \tfrac{1}{4}k_\alpha^2]^{1/2}} \tag{66}$$

and complete the final integral with aid from the identity

$$\frac{1}{[a(1-t^2)+b]^{1/2}} = \frac{1}{ia^{1/2}} \frac{\partial}{\partial t} \mathrm{Ln}\left(2ia^{1/2}t + 2[a(1-t^2)+b]^{1/2}\right), \tag{67}$$

noting, importantly, that if $\mathrm{Im}[a] > 0$ and $\mathrm{Im}[b] = 0$, then the argument of the principal logarithm in Eq. (67) maintains a positive imaginary part for all $t \in [0, k_\alpha/(2k_R)]$. We have now reduced the original double integral to

$$\frac{2i}{[k_E^2 - k_R^2 + i\acute{U}_2]^{1/2}} \left[\mathrm{Ln}\left(i\tfrac{k_\alpha}{2k_R}[k_E^2 - k_R^2 + i\acute{U}_2]^{1/2} + |c_\alpha|[k_E^2 + i\acute{U}_2]^{1/2} \right) - \mathrm{Ln}\left([k_E^2 - \tfrac{1}{4}k_\alpha^2 + i\acute{U}_2]^{1/2}\right) - i\varphi_\alpha^{\max} \right] \tag{68}$$

and we may assemble a near-final result by replacing the integrals in Eq. (61) with this expression.

To conclude the derivation, one performs the $\acute{U} \to 0^+$ limit. Numerous simplifications arise during this process, aided by the identity $\mathrm{sgn}(c_\alpha)\varphi_\alpha^{\max} = \theta_a - \pi h(-c_\alpha)$, the fact that $\theta_1 + \theta_2 + \theta_3 = \pi$, the factorization

$$(4k_E^2 - k_\alpha^2) = \left(2c_\alpha k_E + k_\alpha[1 + \tfrac{k_E^2}{k_R^2}]^{1/2}\right)\left(2c_\alpha k_E - k_\alpha[1 + \tfrac{k_E^2}{k_R^2}]^{1/2}\right), \tag{69}$$

and various properties of the principal logarithm and arctangent functions. For the case when $E < v_0$, we obtain

$$\tilde{H}_2^{E<v_0}(\mathbf{k}_1,\mathbf{k}_2,E) = \frac{2k_R}{\pi k_1 k_2 k_3 [k_R^2 + |\,k_E^2\,|]^{1/2}} \sum_{\alpha=1}^{3} \left[\arctan\left(\frac{2[|\,k_E^2\,|]^{1/2} k_R c_\alpha}{k_\alpha [|\,k_E^2\,|]^{1/2}} \right) - \frac{\pi}{6} \right]; \tag{70}$$

when $0 < k_E < k_R$, we obtain

$$\tilde{H}_2^{0<k_E<k_R}(\mathbf{k}_1,\mathbf{k}_2,E) = \frac{2k_R}{\pi k_1 k_2 k_3 [k_R^2 - k_E^2]^{1/2}} \sum_{\alpha=1}^{3} \left[\begin{array}{l} \frac{\pi}{3} - \pi h(-c_\alpha) - \pi\,\mathrm{sgn}(c_\alpha) h\left(\frac{k_\alpha}{2k_E} [1 - \frac{k_E^2}{k_R^2}]^{1/2} - |c_\alpha| \right) \\ \quad + \frac{\pi}{2}\,\mathrm{sgn}(c_\alpha) h(k_\alpha - 2k_E) + \frac{i}{2} \ln \left| \frac{c_\alpha - \frac{k_\alpha}{2k_E}[1 - \frac{k_E^2}{k_R^2}]^{1/2}}{c_\alpha + \frac{k_\alpha}{2k_E}[1 - \frac{k_E^2}{k_R^2}]^{1/2}} \right| \end{array} \right]; \tag{71}$$

and, finally, when $k_E > k_R$, we obtain

$$\tilde{H}_2^{k_E>k_R}(\mathbf{k}_1,\mathbf{k}_2,E) = \frac{2k_R}{\pi k_1 k_2 k_3 [k_E^2 - k_R^2]^{1/2}} \sum_{\alpha=1}^{3} i \left[\arctan\left(\frac{2c_\alpha k_E k_R}{k_\alpha [k_E^2 - k_R^2]^{1/2}} \right) - \frac{\pi}{6} \right]. \tag{72}$$

The expressions in Eqs. (70)-(72) are the final results for the general case.

Re-considering briefly the case when $\mathbf{k}_1$, $\mathbf{k}_2$, and $\mathbf{k}_3$ form a small equilateral triangle, we see that Eqs. (70) and (72) are the relevant expressions; one may verify that both behave asymptotically as Eq. (53), as expected.

Simplified case: When $\mathbf{k}_1$ and $\mathbf{k}_2$ are collinear

Recalling that $k_R \to \infty$ as $\mathbf{k}_1$ and $\mathbf{k}_2$ become collinear, we may extract the result for this case directly from Eqs. (70) and (71):

$$\tilde{H}_2^{\text{collinear}}(\mathbf{k}_1,\mathbf{k}_2,E) = \frac{2}{\pi k_1 k_2 k_3} \sum_{\alpha=1}^{3} \left\{ \begin{array}{ll} \arctan\left(\frac{2[|\,k_E^2\,|]^{1/2} c_\alpha}{k_\alpha} \right) - \frac{\pi}{6} & E < v_0 \\ -c_\alpha \frac{\pi}{2} h(k_\alpha - 2k_E) + c_\alpha \frac{i}{2} \ln \left| \frac{k_\alpha - 2k_E}{k_\alpha + 2k_E} \right| & E > v_0 \end{array} \right\}, \tag{73}$$

where we have used the fact that $c_\alpha \to \pm 1$ in this limit to simplify the expressions.

IV. RESPONSE FUNCTIONALS FOR THE LOCAL DENSITY OF STATES, ELECTRON DENSITY, AND KINETIC ENERGY DENSITY

Here, we give first- and second-order corrections to the free-electron LDOS, electron density, and electron KED as functionals of the perturbing potential, providing for the first time the reciprocal-space response functions for the KED. By direct Fourier transformation, it is manageable to convert between the (known) real-space and (generally unknown) reciprocal-space response functions *only* at first order. The formulas we give are obtained instead by application of the techniques described in the previous section. The first-order formulas emerge when Eqs. (27)-(29), which originate from Eqs. (4)-(6), are applied to the first-order response function for the equal-position Green function given by Eqs. (32) and (38). The second-order formulas are generated by applying Eqs. (27)-(29) to the second-order response function for the equal-position Green function given by Eqs. (41), (44), (70)-(72), and (73).

The first-order response functions involve a single wave vector, $\mathbf{k}_1$, and it proves convenient to define the dimensionless vector $\boldsymbol{\eta}_1$, which re-scales $\mathbf{k}_1$ by $2k_E$ or $2k_\mu$, depending on context: $\boldsymbol{\eta}_1 = \mathbf{k}_1/(2k_E)$ in the functions involving E, whereas $\boldsymbol{\eta}_1 = \mathbf{k}_1/(2k_\mu)$ in the functions involving μ. The second-order response functions involve two wave vectors, $\mathbf{k}_1$ and $\mathbf{k}_2$, and depend on their lengths as well as the angle between them or, equivalently, the length of $\mathbf{k}_3 = -(\mathbf{k}_1 + \mathbf{k}_2)$, as introduced earlier. Readers who skipped Section III should review the paragraph on the triangle formed by $\mathbf{k}_1$, $\mathbf{k}_2$, and $\mathbf{k}_3$, particularly the definitions of the circumradius k_R and the cosines $\{c_\alpha\}$ given in Eqs. (45) and (46), respectively. We again make use of scaled wave vectors for the second-order case — $\boldsymbol{\eta}_2$ refers to $\mathbf{k}_2/(2k_E)$ or $\mathbf{k}_2/(2k_\mu)$, and likewise for $\boldsymbol{\eta}_3$ — and we utilize a dimensionless circumradius defined by $\zeta_R = k_R/k_E$ or $\zeta_R = k_R/k_\mu$, as well as the following dimensionless quantity,

$$\Delta_R = \sqrt{\left|1 - \frac{k_E^2}{k_R^2}\right|} \qquad \text{or} \qquad \Delta_R = \sqrt{\left|1 - \frac{k_\mu^2}{k_R^2}\right|}, \tag{74}$$

all depending on context.

Finally, we also express the response functions themselves in a dimensionless form, scaled by their respective values for the case when all wave vector arguments are zero. These latter values are given by Eqs. (76), (79), (82), (85), (90), and (95) below—all of which we anticipated in Eq. (11).

First-order response

Local density of states

The first-order change in the LDOS, $\rho_1(\mathbf{r},E)$, is zero if $E<v_0$, as discussed above. Otherwise, it may be expressed as a functional of the real-space potential — see Eqs. (15)-(16) — or as a functional of the Fourier-transformed potential,

$$\rho_1(\mathbf{r},E)=\int\frac{\mathrm{d}\mathbf{k}_1}{(2\pi)^3}e^{i\mathbf{k}_1\cdot\mathbf{r}}\tilde{I}_1(\mathbf{k}_1,k_E)\tilde{v}_\Delta(\mathbf{k}_1)\,, \tag{75}$$

with

$$\tilde{I}_1(0,k_E)=-\frac{1}{\pi^2 k_E} \tag{76}$$

and

$$\frac{\tilde{I}_1(\mathbf{k}_1,k_E)}{\tilde{I}_1(0,k_E)}=\frac{1}{2\eta_1}\ln\left|\frac{1+\eta_1}{1-\eta_1}\right|. \tag{77}$$

The dimensionless function given by Eq. (77) is plotted in Fig. 3(a). It may be obtained by differentiating the static Lindhard function[11] presented next.

Electron density

The first-order response of the electron density, nonzero for $\mu>v_0$, is given in real-space form by Eqs. (15) and (17). The same quantity expressed as a functional of the Fourier-transformed potential is

$$n_1(\mathbf{r})=\int\frac{\mathrm{d}\mathbf{k}_1}{(2\pi)^3}e^{i\mathbf{k}_1\cdot\mathbf{r}}\tilde{J}_1(\mathbf{k}_1,k_\mu)\tilde{v}_\Delta(\mathbf{k}_1), \tag{78}$$

with

$$\tilde{J}_1(0,k_\mu)=-\frac{k_\mu}{\pi^2} \tag{79}$$

and

$$\frac{\tilde{J}_1(\mathbf{k}_1,k_\mu)}{\tilde{J}_1(0,k_\mu)}=\frac{1}{2}+\frac{1-\eta_1^2}{4\eta_1}\ln\left|\frac{1+\eta_1}{1-\eta_1}\right|. \tag{80}$$

As mentioned, $\tilde{J}_1(\mathbf{k}_1,k_\mu)$ is the Lindhard response function[11] for static external potentials. We plot Eq. (80) in Fig. 3(b).

Kinetic energy density

The first-order potential functional for the KED, for $\mu > v_0$, is given either by Eq. (15) with Eq. (18), or by

$$t_1(\mathbf{r}) = \int \frac{\mathbf{d}\mathbf{k}_1}{(2\pi)^3} e^{i\mathbf{k}_1\cdot\mathbf{r}} \tilde{K}_1(\mathbf{k}_1, k_\mu) \tilde{v}_\Delta(\mathbf{k}_1), \tag{81}$$

with

$$\tilde{K}_1(0, k_\mu) = -\frac{k_\mu^3}{2\pi^2} \tag{82}$$

and

$$\frac{\tilde{K}_1(\mathbf{k}_1, k_\mu)}{\tilde{K}_1(0, k_\mu)} = \frac{3}{4} - \frac{3\eta_1^2}{4} + \frac{(1-3\eta_1^2)(1-\eta_1^2)}{8\eta_1} \ln\left|\frac{1+\eta_1}{1-\eta_1}\right| . \tag{83}$$

A plot of Eq. (83) is given in Fig. 3(c). To the best of our knowledge, this function has not been reported before, although it is closely related to the companion functions for the LDOS and the electron density. The first-order response function for the Laplacian version of the KED (see the Appendix) is obtained by adding $k_1^2 \tilde{J}_1(\mathbf{k}_1, k_\mu)/4$ to the response function given here.

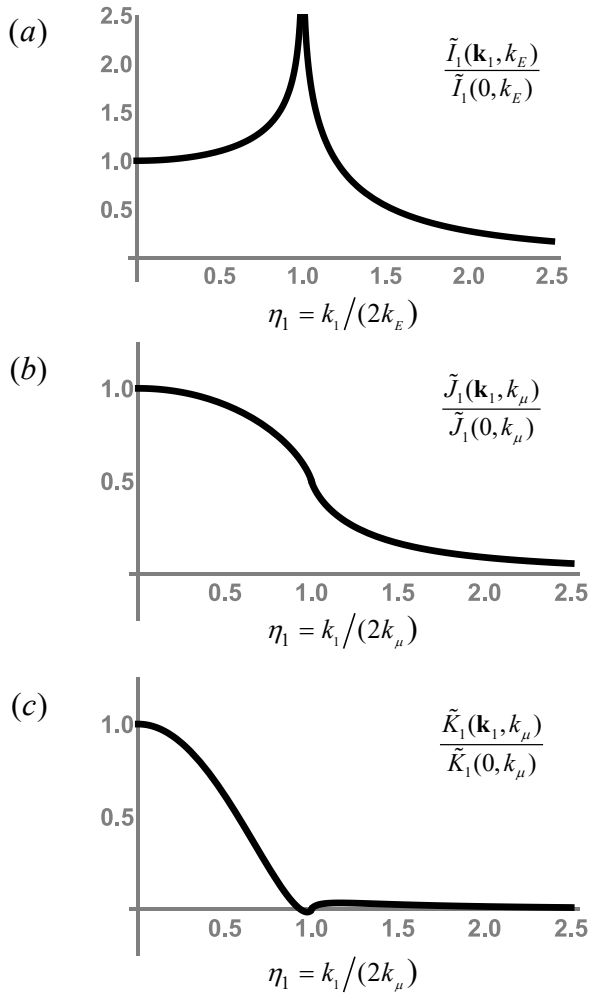

FIG. 3. Dimensionless response functions governing the first-order changes in *(a)* the local density of states, *(b)* the electron density, *(c)* the kinetic energy density, all when expressed as functionals of the perturbing potential. The horizontal axes are normalized by factors of k_E or k_μ, as appropriate, which are wave vectors associated with E or μ, respectively — see the main text for definitions. In the limit of a slowly varying perturbation ($\eta_1 \to 0$), the first-order corrections to the Thomas-Fermi potential functionals are recovered [see Eq. (11)]. The response functions all have a nonanalytic feature (at $\eta_1 = 1$) and decay to zero for the case of a rapidly varying perturbation ($\eta_1 \to \infty$).

Second-order response

Local density of states

The second-order change in the LDOS, $\rho_2(\mathbf{r},E)$, is zero if $E<v_0$, as discussed above. Again, it may be expressed as a functional of the real-space potential — see Eqs. (15)-(16) — or as a functional of the Fourier-transformed potential,

$$\rho_2(\mathbf{r},E)=\int\frac{\mathrm{d}\mathbf{k}_1}{(2\pi)^3}\int\frac{\mathrm{d}\mathbf{k}_2}{(2\pi)^3}e^{i(\mathbf{k}_1+\mathbf{k}_2)\cdot\mathbf{r}}\tilde{I}_2(\mathbf{k}_1,\mathbf{k}_2,k_E)\tilde{v}_\Delta(\mathbf{k}_1)\tilde{v}_\Delta(\mathbf{k}_2)\cdot \tag{84}$$

The function $\tilde{I}_2(\mathbf{k}_1,\mathbf{k}_2,k_E)$, equivalent to a function first obtained by Lloyd and Sholl,[15] is more complicated than its first-order counterpart. When both $\mathbf{k}_1$ and $\mathbf{k}_2$ are zero,

$$\tilde{I}_2(0,0,k_E)=-\frac{1}{2\pi^2k_E^3}; \tag{85}$$

when one of the wave vector arguments is zero, or when $\mathbf{k}_2=-\mathbf{k}_1$,

$$\frac{\tilde{I}_2(\mathbf{k}_1,0,k_E)}{\tilde{I}_2(0,0,k_E)}=\frac{\tilde{I}_2(0,\mathbf{k}_1,k_E)}{\tilde{I}_2(0,0,k_E)}=\frac{\tilde{I}_2(\mathbf{k}_1,-\mathbf{k}_1,k_E)}{\tilde{I}_2(0,0,k_E)}=\frac{1}{1-\eta_1^2}; \tag{86}$$

when $\mathbf{k}_1$ and $\mathbf{k}_2$ are nonzero and collinear, but $\mathbf{k}_2\neq-\mathbf{k}_1$,

$$\frac{\tilde{I}_2^{\text{collinear}}(\mathbf{k}_1,\mathbf{k}_2,k_E)}{\tilde{I}_2(0,0,k_E)}=-\frac{1}{\eta_1\eta_2\eta_3}\sum_{\alpha=1}^{3}c_\alpha\frac{1}{2}\ln\left|\frac{1+\eta_\alpha}{1-\eta_\alpha}\right|; \tag{87}$$

and, finally, when $\mathbf{k}_1$ and $\mathbf{k}_2$ are non-collinear,

$$\frac{\tilde{I}_2(\mathbf{k}_1,\mathbf{k}_2,k_E)}{\tilde{I}_2(0,0,k_E)}=-\frac{1}{\eta_1\eta_2\eta_3\Delta_R}\sum_{\alpha=1}^{3}\begin{cases}\dfrac{1}{2}\ln\left|\dfrac{c_\alpha+\eta_\alpha\Delta_R}{c_\alpha-\eta_\alpha\Delta_R}\right| & k_E<k_R\\ \dfrac{\pi}{6}-\arctan\left(\dfrac{c_\alpha}{\eta_\alpha\Delta_R}\right) & k_E>k_R\end{cases}. \tag{88}$$

The dimensionless version of $\tilde{I}_2(\mathbf{k}_1,\mathbf{k}_2,k_E)$, the expression in Eq. (88), is plotted in Fig. 4 for the cases when the angle between $\mathbf{k}_1$ and $\mathbf{k}_2$ is $\pi/3$ and when it is $2\pi/3$; these two choices subdivide evenly the set of possible angles ranging from zero to π.

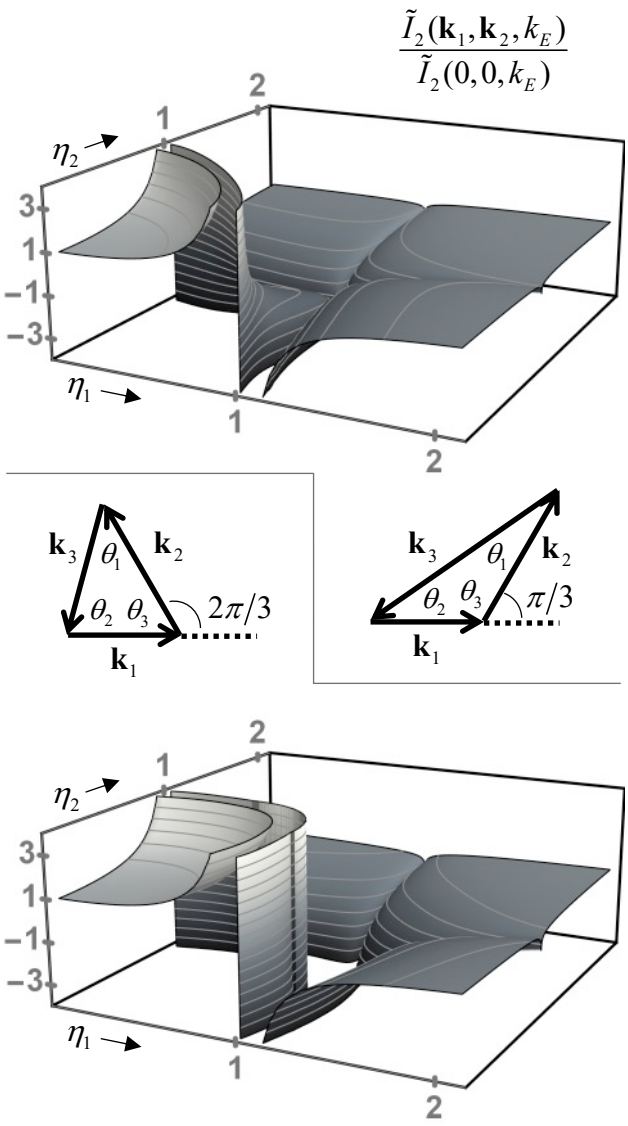

FIG. 4. Plots of the dimensionless response function [Eqs. (86)-(88)] that governs the second-order change in the local density of states when expressed as a functional of the perturbing potential. η_1 and η_2 are scaled lengths (see main text) of the wave vectors $\mathbf{k}_1$ and $\mathbf{k}_2$, respectively. Plotted for the cases when the angle between $\mathbf{k}_1$ and $\mathbf{k}_2$ is $\pi/3$ (top) and when this angle is $2\pi/3$ (bottom). See main text for discussion of the triangle with side lengths k_1, k_2, and $k_3 = |\mathbf{k}_1 + \mathbf{k}_2|$. The second-order correction to the associated Thomas-Fermi functional [see Eq. (11)] is recovered in the $\eta_1, \eta_2 \to 0$ limit and the response function becomes zero in the $\eta_1, \eta_2 \to \infty$ limit.

Electron density

The second-order response of the electron density, nonzero for $\mu > v_0$, is given in real-space form by Eqs. (15) and (17). The same quantity expressed as a functional of the Fourier-transformed potential is

$$n_2(\mathbf{r}) = \int \frac{\mathrm{d}\mathbf{k}_1}{(2\pi)^3} \int \frac{\mathrm{d}\mathbf{k}_2}{(2\pi)^3} e^{i(\mathbf{k}_1+\mathbf{k}_2)\cdot\mathbf{r}} \tilde{J}_2(\mathbf{k}_1,\mathbf{k}_2,k_\mu)\tilde{v}(\mathbf{k}_1)\tilde{v}(\mathbf{k}_2). \tag{89}$$

The earliest derivation of $\tilde{J}_2(\mathbf{k}_1,\mathbf{k}_2,k_\mu)$ is that of Lloyd and Sholl,[15] and a range of seemingly equivalent functions have been derived numerous authors.[17,19,21,24] We compare some of these expressions in the SM. Lloyd and Sholl showed that, when both $\mathbf{k}_1$ and $\mathbf{k}_2$ are zero,

$$\tilde{J}_2(0,0,k_\mu) = \frac{1}{2\pi^2 k_\mu}; \tag{90}$$

when one of the wave vector arguments is zero, or when $\mathbf{k}_2 = -\mathbf{k}_1$,

$$\frac{\tilde{J}_2(\mathbf{k}_1,0,k_\mu)}{\tilde{J}_2(0,0,k_\mu)} = \frac{\tilde{J}_2(0,\mathbf{k}_1,k_\mu)}{\tilde{J}_2(0,0,k_\mu)} = \frac{\tilde{J}_2(\mathbf{k}_1,-\mathbf{k}_1,k_\mu)}{\tilde{J}_2(0,0,k_\mu)} = \frac{1}{2\eta_1}\ln\left|\frac{1+\eta_1}{1-\eta_1}\right|; \tag{91}$$

when $\mathbf{k}_1$ and $\mathbf{k}_2$ are nonzero and collinear, but $\mathbf{k}_2 \neq -\mathbf{k}_1$,

$$\frac{\tilde{J}_2^{\text{collinear}}(\mathbf{k}_1,\mathbf{k}_2,k_\mu)}{\tilde{J}_2(0,0,k_\mu)} = \frac{1}{\eta_1\eta_2\eta_3}\sum_{\alpha=1}^{3} c_\alpha\eta_\alpha\left[\frac{1}{2} + \frac{1-\eta_\alpha^2}{4\eta_\alpha}\ln\left|\frac{1+\eta_\alpha}{1-\eta_\alpha}\right|\right]; \tag{92}$$

and, finally, when $\mathbf{k}_1$ and $\mathbf{k}_2$ are non-collinear,

$$\begin{aligned}\frac{\tilde{J}_2(\mathbf{k}_1,\mathbf{k}_2,k_\mu)}{\tilde{J}_2(0,0,k_\mu)} = {} & \frac{\zeta_R^2}{\eta_1\eta_2\eta_3}\sum_{\alpha=1}^{3} c_\alpha \frac{1}{2}\ln\left|\frac{1+\eta_\alpha}{1-\eta_\alpha}\right| \\ & -\frac{\zeta_R^2\Delta_R}{\eta_1\eta_2\eta_3}\sum_{\alpha=1}^{3}\begin{cases} \dfrac{1}{2}\ln\left|\dfrac{c_\alpha+\eta_\alpha\Delta_R}{c_\alpha-\eta_\alpha\Delta_R}\right| & k_\mu < k_R \\ \arctan\left(\dfrac{c_\alpha}{\eta_\alpha\Delta_R}\right) - \dfrac{\pi}{6} & k_\mu > k_R \end{cases}.\end{aligned} \tag{93}$$

Plots of the dimensionless version of $\tilde{J}_2(\mathbf{k}_1,\mathbf{k}_2,k_\mu)$ are given in Fig. 5.

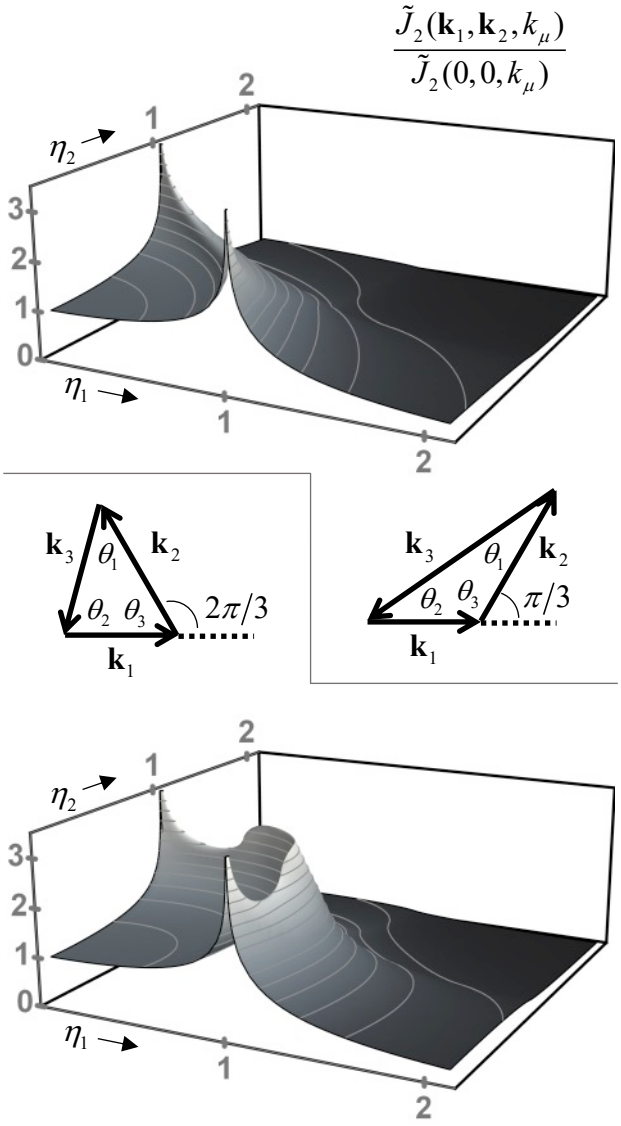

FIG. 5. Plots of the dimensionless response function [Eqs. (91)-(93)] that governs the second-order change in the electron density when expressed as a functional of the perturbing potential. η_1 and η_2 are scaled lengths (see main text) of the wave vectors $\mathbf{k}_1$ and $\mathbf{k}_2$, respectively. Plotted for the cases when the angle between $\mathbf{k}_1$ and $\mathbf{k}_2$ is $\pi/3$ (top) and when this angle is $2\pi/3$ (bottom). See main text for discussion of the triangle with side lengths k_1, k_2, and $k_3 = |\mathbf{k}_1 + \mathbf{k}_2|$. The second-order correction to the associated Thomas-Fermi functional [see Eq. (11)] is recovered in the $\eta_1, \eta_2 \to 0$ limit and the response function becomes zero in the $\eta_1, \eta_2 \to \infty$ limit.

Kinetic energy density

Finally, the second-order potential functional for the KED, for $\mu > v_0$, is given either by Eq. (15) with Eq. (18), or by

$$t_2(\mathbf{r}) = \int \frac{\mathrm{d}\mathbf{k}_1}{(2\pi)^3} \int \frac{\mathrm{d}\mathbf{k}_2}{(2\pi)^3} e^{i(\mathbf{k}_1+\mathbf{k}_2)\cdot\mathbf{r}} \tilde{K}_2(\mathbf{k}_1,\mathbf{k}_2,k_\mu)\tilde{v}(\mathbf{k}_1)\tilde{v}(\mathbf{k}_2). \tag{94}$$

When both $\mathbf{k}_1$ and $\mathbf{k}_2$ are zero,

$$\tilde{K}_2(0,0,k_\mu) = \frac{3k_\mu}{4\pi^2}; \tag{95}$$

when one of the wave vector arguments is zero,

$$\frac{\tilde{K}_2(\mathbf{k}_1,0,k_\mu)}{\tilde{K}_2(0,0,k_\mu)} = \frac{\tilde{K}_2(0,\mathbf{k}_1,k_\mu)}{\tilde{K}_2(0,0,k_\mu)} = \frac{2}{3} + \frac{1-2\eta_1^2}{6\eta_1}\ln\left|\frac{1+\eta_1}{1-\eta_1}\right|; \tag{96}$$

when $\mathbf{k}_2 = -\mathbf{k}_1$,

$$\frac{\tilde{K}_2(\mathbf{k}_1,-\mathbf{k}_1,k_\mu)}{\tilde{K}_2(0,0,k_\mu)} = \frac{1}{3} + \frac{2-\eta_1^2}{6\eta_1}\ln\left|\frac{1+\eta_1}{1-\eta_1}\right|; \tag{97}$$

when $\mathbf{k}_1$ and $\mathbf{k}_2$ are nonzero and collinear, but $\mathbf{k}_2 \neq -\mathbf{k}_1$,

$$\begin{aligned}\frac{\tilde{K}_2^{\text{collinear}}(\mathbf{k}_1,\mathbf{k}_2,k_\mu)}{\tilde{K}_2(0,0,k_\mu)} = {} & \frac{1}{\eta_1\eta_2\eta_3}\sum_{\alpha=1}^{3} c_\alpha \eta_\alpha \left[\frac{1+3\eta_\alpha^2}{36} + \frac{1-\eta_\alpha^4}{24\eta_\alpha}\ln\left|\frac{1+\eta_\alpha}{1-\eta_\alpha}\right|\right] \\ & + \frac{2}{3}\frac{\tilde{J}_1(\mathbf{k}_1,k_\mu)}{\tilde{J}_1(0,k_\mu)} + \frac{2}{3}\frac{\tilde{J}_1(\mathbf{k}_2,k_\mu)}{\tilde{J}_1(0,k_\mu)} - \frac{2\eta_3^2}{3}\frac{\tilde{J}_2(\mathbf{k}_1,\mathbf{k}_2,k_\mu)}{\tilde{J}_2(0,0,k_\mu)}\end{aligned}; \tag{98}$$

and, finally, when $\mathbf{k}_1$ and $\mathbf{k}_2$ are non-collinear,

$$\begin{aligned}\frac{\tilde{K}_2(\mathbf{k}_1,\mathbf{k}_2,k_\mu)}{\tilde{K}_2(0,0,k_\mu)} = {} & -\frac{\zeta_R^2}{\eta_1\eta_2\eta_3}\sum_{\alpha=1}^{3} c_\alpha \left[\frac{\eta_\alpha}{9} - \frac{\eta_\alpha^2+2\zeta_R^2}{18}\ln\left|\frac{1+\eta_\alpha}{1-\eta_\alpha}\right|\right] \\ & - \frac{\zeta_R^2\Delta_R}{\eta_1\eta_2\eta_3}\frac{1+2\zeta_R^2}{9}\sum_{\alpha=1}^{3}\begin{cases} \frac{1}{2}\ln\left|\frac{c_\alpha+\eta_\alpha\Delta_R}{c_\alpha-\eta_\alpha\Delta_R}\right| & k_\mu < k_R \\ \arctan\left(\frac{c_\alpha}{\eta_\alpha\Delta_R}\right) - \frac{\pi}{6} & k_\mu > k_R \end{cases} \\ & + \frac{2}{3}\frac{\tilde{J}_1(\mathbf{k}_1,k_\mu)}{\tilde{J}_1(0,k_\mu)} + \frac{2}{3}\frac{\tilde{J}_1(\mathbf{k}_2,k_\mu)}{\tilde{J}_1(0,k_\mu)} - \frac{2\eta_3^2}{3}\frac{\tilde{J}_2(\mathbf{k}_1,\mathbf{k}_2,k_\mu)}{\tilde{J}_2(0,0,k_\mu)}\end{aligned}. \tag{99}$$

Plots of the dimensionless version of $\tilde{K}_2(\mathbf{k}_1,\mathbf{k}_2,k_\mu)$ are shown in Fig. 6. This function is a central contribution of this work. The second-order response function for the Laplacian definition of the KED (see the Appendix) is obtained by adding $k_3^2\tilde{J}_2(\mathbf{k}_1,\mathbf{k}_2,k_\mu)/4$ to the response function given here.

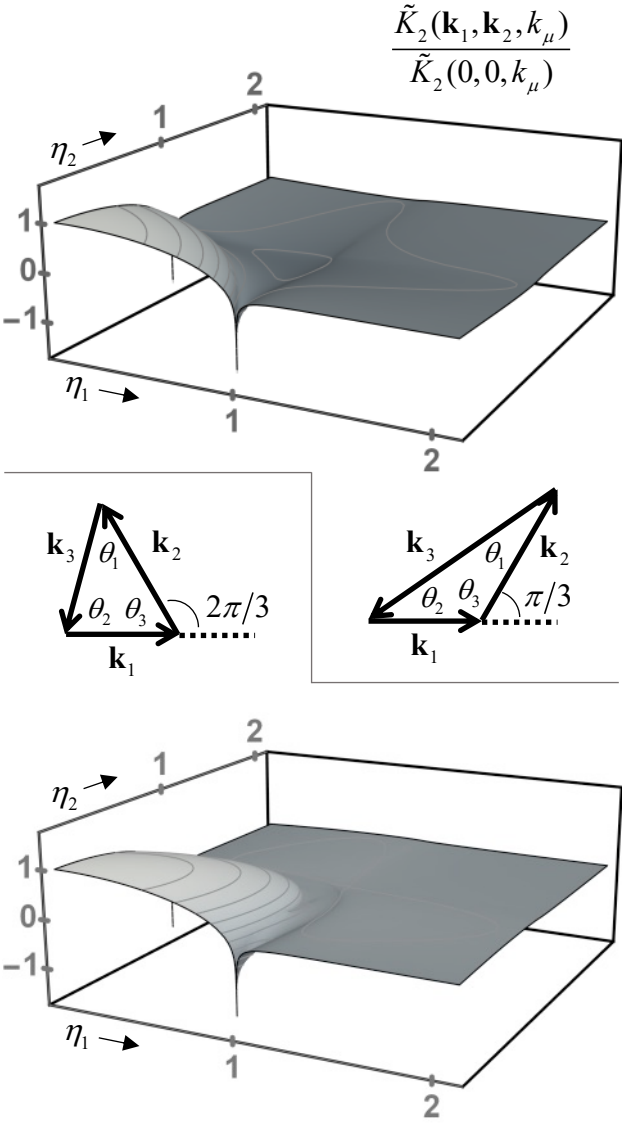

FIG. 6. Plots of the dimensionless response function [Eqs. (96)-(99)] that governs the second-order change in the kinetic energy density when expressed as a functional of the perturbing potential. η_1 and η_2 are scaled lengths (see main text) of the wave vectors $\mathbf{k}_1$ and $\mathbf{k}_2$, respectively. Plotted for the cases when the angle between $\mathbf{k}_1$ and $\mathbf{k}_2$ is $\pi/3$ (top) and when this angle is $2\pi/3$ (bottom). See main text for discussion of the

triangle with side lengths k_1, k_2, and $k_3 = |\mathbf{k}_1 + \mathbf{k}_2|$. The second-order correction to the associated Thomas-Fermi functional [see Eq. (11)] is recovered in the $\eta_1, \eta_2 \to 0$ limit and the response function becomes zero in the $\eta_1, \eta_2 \to \infty$ limit.

V. VALIDATION OF THE RESPONSE FUNCTIONS

The response functions provided in Section IV, particularly those at second order, are somewhat inscrutable, and readers uninterested in replicating the lengthy derivations may wonder if the expressions are entirely correct. Moreover, if the formulas are to be used in numerical work and not just for insight, errant factors of π (for example) could be ruinous. Finally, as we have mentioned previously, several independent formulations of $\tilde{J}_2(\mathbf{k}_1, \mathbf{k}_2, k_\mu)$ appear in the literature and while the competing formulas are all similar in structure, they do not agree in every particular. One presumes they are equivalent — the space of possible rearrangements of the logarithms and arctangents is large — but it is still useful to compare various candidates with a known benchmark. To this end, we describe a multi-part validation strategy involving: (1) study of a nontrivial asymptotic condition (introduced already, the case when k_1, k_2, and k_3 form a small equilateral triangle); (2) a demonstration showing that the response function formalism recovers known gradient expansions for slowly varying potentials; (3) numerical calculation of the response functions themselves; and (4) consideration of the linear potential model system.

The first three components of the validation effort start from the same point. Based on Eqs. (27) -(29) and the modified integral form for $\tilde{H}_2(\mathbf{k}_1, \mathbf{k}_2, E)$ given by Eq. (50), we construct new integral representations for the response functions of interest (in dimensionless form):

$$\frac{\tilde{I}_2(\mathbf{k}_1, \mathbf{k}_2, k_E)}{\tilde{I}_2(0,0,k_E)} = 2 \lim_{\eta_2 \to 0^+} \mathrm{Re} \int_0^1 dx \int_0^1 dy \frac{h(1-x-y)}{[1 - 4x\eta_1^2 - 4y\eta_3^2 + 4 \| x\boldsymbol{\eta}_1 - y\boldsymbol{\eta}_3 \|^2 + i\eta_2]^{3/2}}, \tag{100}$$

$$\frac{\tilde{J}_2(\mathbf{k}_1, \mathbf{k}_2, k_\mu)}{\tilde{J}_2(0,0,k_\mu)} = 2 \lim_{\eta_2 \to 0^+} \mathrm{Re} \int_0^1 dx \int_0^1 dy \frac{h(1-x-y)}{[1 - 4x\eta_1^2 - 4y\eta_3^2 + 4 \| x\boldsymbol{\eta}_1 - y\boldsymbol{\eta}_3 \|^2 + i\eta_2]^{1/2}}, \tag{101}$$

and

$$\begin{aligned} \frac{\tilde{K}_2(\mathbf{k}_1, \mathbf{k}_2, k_\mu)}{\tilde{K}_2(0,0,k_\mu)} &= \frac{1 - 2\eta_3^2}{3} \frac{\tilde{J}_2(\mathbf{k}_1, \mathbf{k}_2, k_\mu)}{\tilde{J}_2(0,0,k_\mu)} + \frac{2}{3} \left[\frac{\tilde{J}_1(\mathbf{k}_1, k_\mu)}{\tilde{J}_1(0,k_\mu)} + \frac{\tilde{J}_1(\mathbf{k}_2, k_\mu)}{\tilde{J}_1(0,k_\mu)} \right] \\ &- \frac{4}{3} \lim_{\eta_2 \to 0^+} \mathrm{Re} \int_0^1 dx \int_0^1 dy\, h(1-x-y) \left[1 - 4x\eta_1^2 - 4y\eta_3^2 + 4 \| x\boldsymbol{\eta}_1 - y\boldsymbol{\eta}_3 \|^2 + i\eta_2 \right]^{1/2} \end{aligned} . \tag{102}$$

The energy integrals required by Eqs. (28)-(29) are facilitated by the observation that both integrands become purely imaginary in the $\epsilon \to 0^+$ limit as E tends to $-\infty$. The specific form of Eq. (102) is obtained from the second line of Eq. (29).

The integrals in Eqs. (100)-(102) are exact restatements of the respective response functions, lightly manipulated into a convenient form, but otherwise untainted by repeated transformations that might introduce error. Having unified denominators and simple, finite domains, they are amenable to asymptotic analysis and well-suited to numerical treatment, which we pursue in turn.

Asymptotic case: When $\mathbf{k}_1$, $\mathbf{k}_2$, and $\mathbf{k}_3$ form a small equilateral triangle

Assuming that k_1, k_2, and k_3 each have length l, we analyze the small-l behavior of Eqs. (100)-(102) exactly as in Section III, obtaining

$$\frac{\tilde{I}_2^{\text{equilateral}}(l \to 0, k_E)}{\tilde{I}_2(0,0,k_E)} \approx 1 + \frac{3}{2}\eta_l^2 + 2\eta_l^4, \tag{103}$$

$$\frac{\tilde{J}_2^{\text{equilateral}}(l \to 0, k_\mu)}{\tilde{J}_2(0,0,k_\mu)} \approx 1 + \frac{1}{2}\eta_l^2 + \frac{2}{5}\eta_l^4, \tag{104}$$

and

$$\frac{\tilde{K}_2^{\text{equilateral}}(l \to 0, k_\mu)}{\tilde{K}_2(0,0,k_\mu)} \approx 1 - \frac{11}{18}\eta_l^2 - \frac{1}{5}\eta_l^4, \tag{105}$$

where $\eta_l = l/(2k_E)$ or $\eta_l = l/(2k_\mu)$, depending on context. One may then compare Eqs. (103)-(105) with Taylor series obtained under the same assumptions from Eqs. (88), (93), and (99)—the respective pairs match exactly. We give plots comparing the exact functions with their asymptotic approximations in Fig. 7. The agreement is excellent in each case for $l \ll 1$, building confidence in the second-order formulas. We utilize this analytical tool again in the SM to quickly prescreen expressions for $\tilde{J}_2(\mathbf{k}_1, \mathbf{k}_2, k_\mu)$ found in the literature.

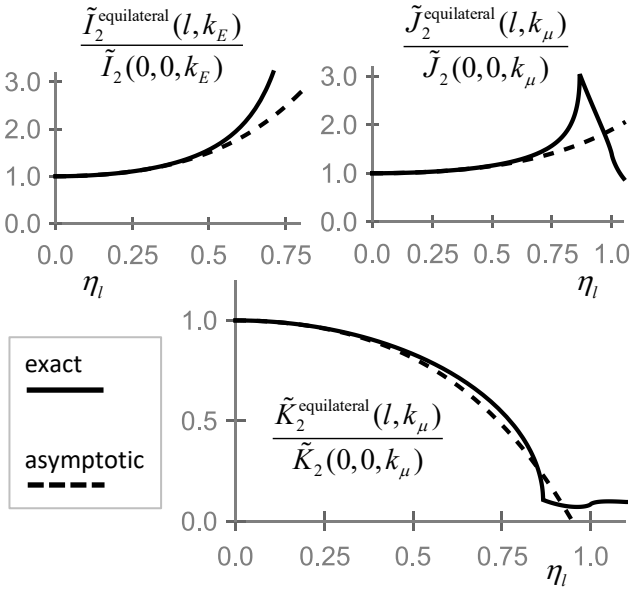

FIG. 7. For the case when $\mathbf{k}_1$, $\mathbf{k}_2$, and $\mathbf{k}_3$ form an equilateral triangle of length l, the second-order response functions for the local density of states (top left), the electron density (top right), and the kinetic energy density (bottom right). Plotted alongside asymptotic approximations derived independently for $l \to 0$; the agreement (in this limit) helps validate the response-function formulas.

Recovering gradient expansions for slowly varying potentials

The response functional formalism can recover the well-studied conventional gradient expansions (see Refs. 38 and 43 and references therein) that are appropriate for slowly varying potentials and may be derived in a variety of ways. Proceeding as in the previous subsection, we may obtain asymptotic forms of the various response functions for $\mathbf{k}_1 \to 0$ and $\mathbf{k}_2 \to 0$, given here for the electron density and KED response functions through fourth order in the wave vectors:

$$\frac{\tilde{J}_1(\mathbf{k}_1 \to 0, k_\mu)}{\tilde{J}_1(0,k_\mu)} \approx 1 - \frac{1}{3}\eta_1^2 - \frac{1}{15}\eta_1^4, \tag{106}$$

$$\frac{\tilde{K}_1(\mathbf{k}_1 \to 0, k_\mu)}{\tilde{K}_1(0,k_\mu)} \approx 1 - \frac{5}{3}\eta_1^2 + \frac{7}{15}\eta_1^4, \tag{107}$$

$$\begin{aligned}\frac{\tilde{J}_2(\mathbf{k}_1 \to 0, \mathbf{k}_2 \to 0, k_\mu)}{\tilde{J}_2(0,0,k_\mu)} &\approx 1 + \frac{1}{3}(\eta_1^2 + \eta_2^2) + \frac{1}{3}\boldsymbol{\eta}_1 \cdot \boldsymbol{\eta}_2 \\ &+ \frac{1}{5}(\eta_1^4 + \eta_2^4) + \frac{4}{15}(\eta_1^2 + \eta_2^2)\boldsymbol{\eta}_1 \cdot \boldsymbol{\eta}_2 + \frac{1}{3}\eta_1^2\eta_2^2 + \frac{2}{15}(\boldsymbol{\eta}_1 + \boldsymbol{\eta}_2)^2 \boldsymbol{\eta}_1 \cdot \boldsymbol{\eta}_2\end{aligned}, \tag{108}$$

and

$$\frac{\tilde{K}_2(\mathbf{k}_1 \to 0, \mathbf{k}_2 \to 0, k_\mu)}{\tilde{K}_2(0,0,k_\mu)} \approx 1 - \frac{5}{9}(\eta_1^2 + \eta_2^2) - \boldsymbol{\eta}_1 \cdot \boldsymbol{\eta}_2 \\ -\frac{7}{45}(\eta_1^4 + \eta_2^4) - \frac{8}{27}(\eta_1^2 + \eta_2^2)\boldsymbol{\eta}_1 \cdot \boldsymbol{\eta}_2 - \frac{7}{27}\eta_1^2\eta_2^2 - \frac{4}{27}(\boldsymbol{\eta}_1 + \boldsymbol{\eta}_2)^2 \boldsymbol{\eta}_1 \cdot \boldsymbol{\eta}_2 \quad . \tag{109}$$

These asymptotic forms permit recovery of the conventional gradient expansions. For example, the gradient expansion for the electron density through second order is

$$n(\mathbf{r}) \to \frac{k_\mu(\mathbf{r})^3}{3\pi^2} - \frac{\nabla^2 v(\mathbf{r})}{12\pi^2 k_\mu(\mathbf{r})} - \frac{|\nabla v(\mathbf{r})|^2}{24\pi^2 k_\mu(\mathbf{r})^3}, \tag{110}$$

which may be obtained from Eqs. (10), (78), (89), (106), and (108), and the analogous gradient expansion for the KED is

$$t(\mathbf{r}) \to \frac{k_\mu(\mathbf{r})^5}{10\pi^2} - \frac{5k_\mu(\mathbf{r})\nabla^2 v(\mathbf{r})}{24\pi^2} + \frac{3|\nabla v(\mathbf{r})|^2}{16\pi^2 k_\mu(\mathbf{r})}, \tag{111}$$

which may be obtained from Eqs. (10), (81), (94), (107), and (109). The fact that this approach yields the same gradient expansions obtained by other means—note that Eqs. (110) and (111), respectively, agree with Eqs. (6.7.17) and (6.7.19) in Ref. 43—provides further evidence that the response functions are correct.

Validation by numerical integration

We defer detailed discussion of the numerical integration to the SM. Note, however, that we have written $\acute{U}_2 \to 0^+$ limits explicitly in each of Eqs. (100)-(102). When performing the integrals numerically, we choose a small, positive value for $\acute{U}_2$ to avoid poles in the integrands. The analysis in the SM confirms that the formulas given in Section IV are correct. We provide code used for this purpose in the form of an open-source Jupyter notebook,[44,45] so that readers may download it and verify this conclusion themselves.

Electrons in a linear potential

To conclude this validation section, we consider noninteracting electrons in the linear potential $v(\mathbf{r}) = g\,\hat{z}$, often referred to as the Airy gas.[46–49] Analytical expressions[49] for the electron density and KED are known for this system:

$$n_{\text{lin}}(\mathbf{r}) = \frac{1}{6\pi l^3}\left[2\zeta^2 \text{Ai}^2(\zeta) - \text{Ai}(\zeta)\text{Ai}'(\zeta) - 2\zeta\,\text{Ai}'^2(\zeta)\right] \tag{112}$$

and

$$t_{\mathrm{lin}}(\mathbf{r}) = \frac{1}{20\pi l^5}\Big[2(1-\zeta^3)\mathrm{Ai}^2(\zeta) + \zeta\,\mathrm{Ai}(\zeta)\mathrm{Ai}'(\zeta) + 2\zeta^2\mathrm{Ai}'^2(\zeta)\Big], \tag{113}$$

where $l = (2g)^{-1/3}$ and $\zeta = -(\mu - gz)/(gl)$. For definiteness, we consider the case of $\mu = 2$ and $g = 1/2$, for which plots of Eqs. (112) and (113) are given in Fig. 8.

To probe the effectiveness of the response functions, we consider the region around $z = 0$ and choose $k_\mu = [2\mu]^{1/2}$ to define an appropriate free-electron reference system for this region. Using the response function formalism along with the Fourier transform $\mathrm{F}[\mathbf{r}] = i(2\pi)^3\nabla_k\delta(\mathbf{k})$, one can show that the electron density in the neighborhood of $z = 0$ is given through second order by

$$\begin{aligned} n(\mathbf{r}) &\approx \frac{k_\mu^3}{3\pi^2} + ig\int \mathrm{d}\mathbf{k}_1 e^{i\mathbf{k}_1\cdot\mathbf{r}}\tilde{J}_1(\mathbf{k}_1,k_\mu)\frac{\partial}{\partial k_z}\delta(\mathbf{k}) \\ &\quad -g^2\int \mathrm{d}\mathbf{k}_1\int \mathrm{d}\mathbf{k}_2 e^{i(\mathbf{k}_1+\mathbf{k}_2)\cdot\mathbf{r}}\tilde{J}_2(\mathbf{k}_1,\mathbf{k}_2,k_\mu)\frac{\partial}{\partial k_{1z}}\delta(\mathbf{k}_1)\frac{\partial}{\partial k_{2z}}\delta(\mathbf{k}_2) \\ &\approx \frac{k_\mu^3}{3\pi^2} + g\tilde{J}_1(0,k_\mu)z + g^2\tilde{J}_2(0,0,k_\mu)z^2 - g^2\frac{\partial^2}{\partial k_{1z}\partial k_{2z}}\tilde{J}_2(\mathbf{k}_1,\mathbf{k}_2,k_\mu)\Big|_{\substack{\mathbf{k}_1=0\\ \mathbf{k}_2=0}} \end{aligned} \tag{114}$$

An analogous treatment for the KED yields

$$t(\mathbf{r}) \approx \frac{k_\mu^5}{10\pi^2} + g\tilde{K}_1(0,k_\mu)z + g^2\tilde{K}_2(0,0,k_\mu)z^2 - g^2\frac{\partial^2}{\partial k_{1z}\partial k_{2z}}\tilde{K}_2(\mathbf{k}_1,\mathbf{k}_2,k_\mu)\Big|_{\substack{\mathbf{k}_1=0\\ \mathbf{k}_2=0}}. \tag{115}$$

Plots of Eqs. (114) and (115) are given in Fig 8, from which it is clear that these approximations effectively describe the exact quantities in the neighborhood of $z = 0$.

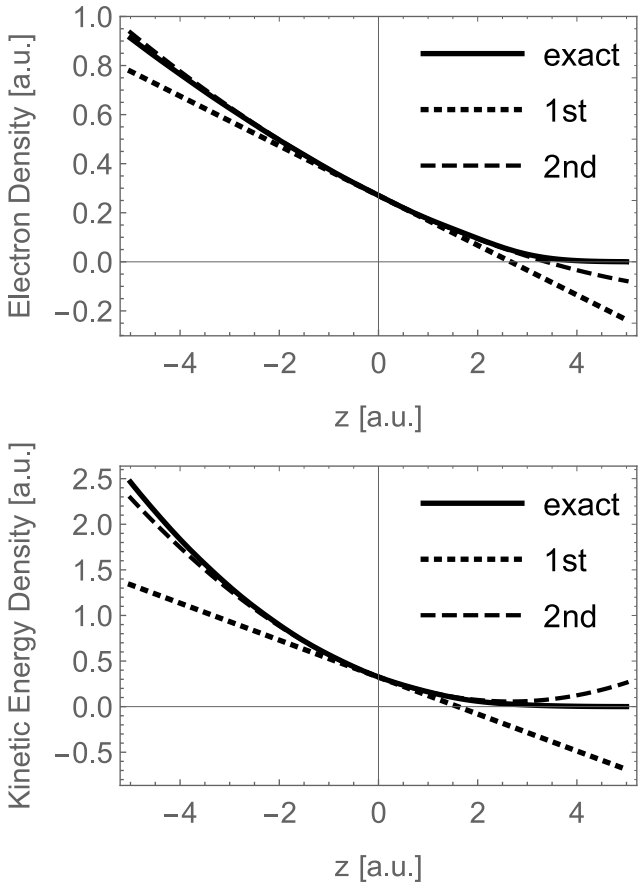

FIG 8. The electron density (top, solid curve) and kinetic energy density (bottom, solid curve) as functions of the position z are shown for the Airy gas model system with $\mu = 2$ and $g = 1/2$. Also shown are response-functional-based approximations through first-order (dotted lines) and second-order (dashed curves) utilizing a free-electron reference system with $k_\mu = [2\mu]^{1/2}$, which is appropriate near $z = 0$.

VI. CONCLUDING REMARKS

In this paper, we considered the local, non-negative KED of initially free electrons perturbed by an external potential. In particular, we derived the reciprocal-space response kernels through second order based on a free-electron reference system. While our treatment of the subject was relatively formal, we use these results in Part II to obtain alternate first- and second-order corrections to the free-electron KED as functionals of the induced electron density—and there we examine the performance of the density functionals when applied local pseudopotential models of crystals.

The reciprocal-space formulas for the first- or second-order response functions for the KED—Eqs. (83) and (96)-(99)—constitute our main results. In view of the complicated form of the second-order function, we employed a multi-part validation strategy to ensure its correctness. Some of this procedure is detailed in Section V, and the remainder is in the SM. In doing so, we showed that several[15,16,21] second-order response functions for the electron density are equivalent, despite apparent differences in form.

VII. ACKNOWLEDGEMENTS

We thank Ms. Nari Baughman and Drs. Beatriz G. del Rio, Xing Zhang, and Kaili Jiang for reviewing versions of this manuscript and acknowledge support from the Office of Naval Research (Grant No. N00014-15-1-2218).

VIII. APPENDIX

Mathematical notes

Throughout, we adhere to the following Fourier transform conventions for three-dimensional functions,

$$\begin{aligned}\tilde{f}(\mathbf{k}) &= \mathrm{F}\left[f(\mathbf{r})\right] = \int \mathrm{d}\mathbf{r}\, e^{-i\mathbf{k}\cdot\mathbf{r}} f(\mathbf{r}) \\ f(\mathbf{r}) &= \mathrm{F}^{-1}\left[\tilde{f}(\mathbf{k})\right] = \int \frac{\mathrm{d}\mathbf{k}}{(2\pi)^3} e^{i\mathbf{k}\cdot\mathbf{r}} \tilde{f}(\mathbf{k})\end{aligned}. \tag{116}$$

We denote plane-wave eigenstates by

$$\langle \mathbf{r}|\mathbf{k}\rangle = \frac{e^{i\mathbf{k}\cdot\mathbf{r}}}{(2\pi)^{3/2}}, \tag{117}$$

meaning that no extra normalizations appear in resolutions of the identity and that

$$\langle \mathbf{k}_1|\hat{v}_\Delta|\mathbf{k}_2\rangle = \frac{\tilde{v}(\mathbf{k}_1-\mathbf{k}_2)}{(2\pi)^3}. \tag{118}$$

The Laplacian version of the kinetic energy density and Eq. (6)

While the KED defined in Eqs. (1) and (6) is useful because it is strictly non-negative, other functions yielding the same total kinetic energy upon integration may also justifiably be called KEDs. The eigenfunctions of the Hamiltonian considered in this paper can be made strictly real, meaning that, after expanding the reduced density matrix in these eigenfunctions and defining $t_L(\mathbf{r}) = -\frac{1}{2}[\nabla_{\mathbf{r}}^2 \gamma(\mathbf{r},\mathbf{r}_0)]_{\mathbf{r}_0\to\mathbf{r}}$, one can show directly using the product rule that

$$t(\mathbf{r}) = t_L(\mathbf{r}) + \tfrac{1}{4}\nabla^2 n(\mathbf{r}). \tag{119}$$

The integral of $\nabla^2 n(\mathbf{r})$ vanishes for systems that are finite or described with periodic boundary conditions, establishing that the two KEDs yield the same total kinetic energy for either case.

Continuing, after noting that

$$\gamma(\mathbf{r},\mathbf{r}_0) = -\tfrac{2}{\pi}\int_{-\infty}^{\mu} \mathrm{Im}G^+(\mathbf{r},\mathbf{r}_0,E)\,\mathrm{d}E\,, \tag{120}$$

it becomes clear that

$$t_L(\mathbf{r}) = -\tfrac{2}{\pi}\int_{-\infty}^{\mu}\left[-\mathrm{Im}\tfrac{1}{2}\nabla_{\mathbf{r}}^2 G^+(\mathbf{r},\mathbf{r}_0,E)\right]_{\mathbf{r}_0\to\mathbf{r}}\mathrm{d}E, \tag{121}$$

from which one begins to see how $t_L(\mathbf{r})$ arises naturally in conjunction with the Schrödinger equation. To obtain the second line of Eq. (6), expand the Hamiltonian in Eq. (3) and use the result to replace the Laplacian term in Eq. (121). Then, after extraction of the imaginary part, the $\acute{U}\to 0^+$ limit, and some simple rearrangement, the expected result follows from Eq. (119).

IX. REFERENCES

[1] R.G. Newton, *Scattering Theory of Waves and Particles*, 2nd ed. (Springer-Verlag, Berlin Heidelberg, 1982).
[2] J.R. Taylor, *Scattering Theory: The Quantum Theory of Nonrelativistic Collisions* (Dover Publications, Mineola, NY, 2006).
[3] W.C. Witt and E.A. Carter, Phys. Rev. B (2019).
[4] J.C. Stoddart and N.H. March, Proc R Soc Lond A **299**, 279 (1967).
[5] Y.A. Wang and E.A. Carter, in *Theor. Methods Condens. Phase Chem.* (Springer, Dordrecht, 2002), pp. 117–184.
[6] T.A. Wesolowski and Y.A. Wang, editors , *Recent Progress in Orbital-Free Density Functional Theory* (World Scientific, Singapore, 2013).
[7] V.V. Karasiev, D. Chakraborty, and S.B. Trickey, in *Many-Electron Approaches Phys. Chem. Math.* (Springer, Cham, 2014), pp. 113–134.
[8] W.C. Witt, B.G. del Rio, J.M. Dieterich, and E.A. Carter, J. Mater. Res. **33**, 777 (2018).
[9] P. Hohenberg and W. Kohn, Phys. Rev. **136**, B864 (1964).
[10] W. Kohn and L.J. Sham, Phys. Rev. **140**, A1133 (1965).
[11] J. Lindhard, K Dan Vidensk Selsk Mat Fys Medd **28**, 1 (1954).
[12] N.H. March and A.M. Murray, Phys. Rev. **120**, 830 (1960).
[13] N.H. March and A.M. Murray, Proc R Soc Lond A **261**, 119 (1961).
[14] N.H. March Young, W.H.&. Sampanthar, S., *The Many-Body Problem in Quantum Mechanics* (Cambridge University Press, 1967).
[15] P. Lloyd and C.A. Sholl, J. Phys. C Solid State Phys. **1**, 1620 (1968).

[16] E.G. Brovman, Yu. Kagan, and A. Kholas, Sov. J. Exp. Theor. Phys. **34**, 394 (1972).
[17] E.G. Brovman and Yu. Kagan, Sov. J. Exp. Theor. Phys. **36**, 1025 (1973).
[18] E.G. Brovman and A. Kholas, Sov. J. Exp. Theor. Phys. **39**, 924 (1974).
[19] J. Hammerberg and N.W. Ashcroft, Phys. Rev. B **9**, 409 (1974).
[20] R. Pickenhain and A. Milchev, Phys. Status Solidi B **77**, 571 (1976).
[21] A. Milchev and R. Pickenhain, Phys. Status Solidi B **79**, 549 (1977).
[22] A. Milchev and K. Unger, Phys. Status Solidi B **87**, 227 (1978).
[23] R. Pickenhain and K. Unger, Phys. Status Solidi B **102**, 611 (1980).
[24] S. Li and J.K. Percus, J. Math. Phys. **32**, 776 (1991).
[25] J.M. Pitarke, R.H. Ritchie, and P.M. Echenique, Phys. Rev. B **52**, 13883 (1995).
[26] N.W. Ashcroft, *Solid State Physics* (Philadelphia: Saunders College, 1976).
[27] M. Finnis, *Interatomic Forces in Condensed Matter* (Oxford University Press, Oxford, New York, 2004).
[28] G. Giuliani, *Quantum Theory of the Electron Liquid* (New York: Cambridge University Press, 2005).
[29] See Supplemental Material at [URL will be inserted by publisher] for additional verification of the response function formulas.
[30] J. Rammer, *Quantum Transport Theory* (Avalon Publishing, Reading, MA, 2004).
[31] E.N. Economou, *Green's Functions in Quantum Physics*, 3rd [expanded] ed. (New York: Springer, 2006).
[32] L.H. Thomas, Math. Proc. Camb. Philos. Soc. **23**, 542 (1927).
[33] E. Fermi, Rend Accad Naz Lincei **6**, 32 (1927).
[34] G. 't Hooft and M. Veltman, Nucl. Phys. B **153**, 365 (1979).
[35] R. Cenni and P. Saracco, Nucl. Phys. A **487**, 279 (1988).
[36] R. Cenni, F. Conte, A. Cornacchia, and P. Saracco, Riv. Nuovo Cimento 1978-1999 **15**, 1 (1992).
[37] L.R. Pratt, G.G. Hoffman, and R.A. Harris, J. Chem. Phys. **88**, 1818 (1988).
[38] R.M. Dreizler and E.K.U. Gross, *Density Functional Theory: An Approach to the Quantum Many-Body Problem* (Springer Science & Business Media, 1990).
[39] J.P. Perdew and S. Kurth, in *Primer Density Funct. Theory*, edited by C. Fiolhais, F. Nogueira, and M.A.L. Marques (Springer Berlin Heidelberg, Berlin, Heidelberg, 2003), pp. 1–55.
[40] S. Gravel and N.W. Ashcroft, Phys. Rev. B **76**, 144103 (2007).
[41] A. Cangi, D. Lee, P. Elliott, K. Burke, and E.K.U. Gross, Phys. Rev. Lett. **106**, 236404 (2011).
[42] C. Cohen-Tannoudji, B. Diu, and F. Laloe, *Quantum Mechanics*, 1 edition (Wiley-VCH, New York, NY, 1992).
[43] R.G. Parr and W. Yang, *Density-Functional Theory of Atoms and Molecules* (Oxford University Press, USA, 1994).
[44] F. Perez and B.E. Granger, Comput. Sci. Eng. **9**, 21 (2007).
[45] T. Kluyver, B. Ragan-Kelley, F. Pérez, B. Granger, M. Bussonnier, J. Frederic, K. Kelley, J. Hamrick, J. Grout, S. Corlay, P. Ivanov, D. Avila, S. Abdalla, and C. Willing, in *Position. Power Acad. Publ. Play. Agents Agendas*, edited by F. Loizides and B. Schmidt (2016), pp. 87–90.
[46] R. Baltin, Phys. Lett. A **37**, 67 (1971).
[47] R. Baltin, Z. Für Naturforschung A **27**, 1176 (1972).
[48] L. Vitos, B. Johansson, J. Kollár, and H.L. Skriver, Phys. Rev. A **61**, 052511 (2000).
[49] A. Lindmaa, A.E. Mattsson, and R. Armiento, Phys. Rev. B **90**, 075139 (2014).